THE JOURNAL OF COMPARATIVE NEUROLOGY 394:186–204 (1998)

Morphological and Electrophysiological Characteristics of Noncholinergic Basal Forebrain Neurons

K. PANG,[1,2]* **J.M. TEPPER,**[1] **AND L. ZABORSZKY**[1]
[1]Center for Molecular and Behavioral Neurosciences, Rutgers, The State University of New Jersey, Newark, New Jersey 07102
[2]Department of Psychology, Bowling Green State University, Bowling Green, Ohio 43403

ABSTRACT

Cholinergic neurons in the basal forebrain are the focus of considerable interest because they are severely affected in Alzheimer's disease. However, both cholinergic and noncholinergic neurons are intermingled in this region. The goal of the present study was to characterize the morphology and in vivo electrophysiology of noncholinergic basal forebrain neurons. Neurons in the ventral pallidum and substantia innominata were recorded extracellularly, labeled juxtacellularly with biocytin and characterized for the presence of choline acetyltransferase immunoreactivity. Two types of ventral pallidal cells were observed. Type I ventral pallidal neurons had axons that rarely branched near the cell body and tended to have smaller somata and lower spontaneous firing rates than did type II ventral pallidal neurons, which displayed extensive local axonal arborizations. Subtypes of substantia innominata neurons could not be distinguished based on axonal morphology. These noncholineregic neurons exhibited local axon arborizations along a continuum that varied from no local collaterals to quite extensive arbors. Substantia innominata neurons had lower spontaneous firing rates, more variable interspike intervals, and different spontaneous firing patterns than did type II ventral pallidal neurons and could be antidromically activated from cortex or substantia nigra, indicating that they were projection neurons. Ventral pallidal neurons resemble, both morphologically and electrophysiologically, previously described neurons in the globus pallidus, whereas the substantia innominata neurons bore similarities to isodendritic neurons of the reticular formation. These results demonstrate the heterogeneous nature of noncholinergic neurons in the basal forebrain. J. Comp. Neurol. 394:186–204, 1998.

Indexing terms: choline acetyltransferase; GABA; biocytin; juxtacellular labeling

The magnocellular basal forebrain cholinergic system has been implicated in a number of important cognitive processes, including learning, memory, attention, and arousal (Robbins et al., 1989; Pang et al., 1993; Muir et al., 1994; Sarter, 1994; Wenk, 1997). In fact, major hypotheses of Alzheimer's disease, Parkinson's disease, and schizophrenia suggest that dysfunction of this system is responsible for some of the cognitive deficits associated with these illnesses (Heimer et al., 1991; Chan-Palay et al., 1993; Geula and Mesulam, 1994; Price et al., 1994). Thus, understanding the basal forebrain cholinergic system and its circuitry is important for the development of therapies to treat these diseases.

The magnocellular basal forebrain complex, comprised of the medial septum, vertical and horizontal limbs of the diagonal band of Broca, ventral pallidum (VP), substantia innominata (SI), globus pallidus, internal capsule, and peripallidal areas, consists of a heterogeneous population of neurons. To date, the population receiving the most interest has been the cholinergic neurons. Much less is known about the morphology and electrophysiological characteristics of noncholinergic neurons in this area. These noncholinergic neurons are mostly gamma-aminobutyric acid (GABA)-ergic and/or peptidergic (Zaborszky et al., 1986a; Walker et al., 1989; Gritti et al., 1993). Some of these neurons are projection neurons, ascending to the

Grant sponsor: NIH; Grant numbers: NS35389, MH52450, NS23945, and NS34865.

*Correspondence to: Dr. Kevin Pang, Department of Psychology, Bowling Green State University, Bowling Green, OH 43403.
E-mail: kpang@bgnet.bgsu.edu

Received 28 August 1996; Revised 12 December 1997; Accepted 17 December 1997

cerebral cortex, hippocampus, olfactory bulb, and thalamic reticular nucleus and descending to the caudal diencephalon and brainstem (Vincent et al., 1983; Zaborszky et al., 1986a; Asanuma and Porter, 1990; Gritti et al., 1994). Others are most likely interneurons, making contact among themselves and with cholinergic neurons in their local vicinity (Zaborszky et al., 1986b; Ingham et al., 1988).

Cholinergic and noncholinergic neurons projecting to the neocortex are located in the VP, SI, globus pallidus, and internal capsule in rodents. This dispersed group of neurons is collectively termed the 'nucleus basalis' in primates. Cytoarchitectonic, hodological, and neurochemical data suggest that the VP and SI belong to separate neural systems (Heimer et al., 1997). In this view, the VP is part of the striatopallidal complex, and the sublenticular SI is considered to be part of the 'extended amygdala' because of its close relationship to the amygdaloid body and the bed nucleus of the stria terminalis.

Because of the limited information available concerning the noncholinergic components of the magnocellular basal forebrain complex, the present study examined the morphological and electrophysiological characteristics of noncholinergic neurons in the VP and SI. For this study, neurons in the VP and ventral globus pallidus were considered to be ventral pallidal neurons and those in the sublenticular SI, internal capsule, and bed nucleus of the stria terminalis were grouped together as SI neurons.

MATERIALS AND METHODS

Subjects

Subjects were 14 male Sprague-Dawley rats (Zivic-Miller, Portersville, PA) and 10 male hooded, Long-Evans rats (Harlan, Indianapolis, IN) weighing 300–400 g at the time of recording. Rats were housed two to a cage, with food and water available ad libitum on a 12-hour light/dark cycle. All recordings were performed during the light phase. All animal procedures were conducted in accordance with the NIH Guide for the Care and Use of Laboratory Animals. The Research Animal Facility at Rutgers University and Bowling Green State University are USDA registered and AAALAC accredited.

Surgery

Rats were anesthetized with urethane (1.5 g/kg, i.p.) and placed in a stereotaxic instrument. Body temperature was maintained at 37°C ± 1 by a heating pad. The scalp and overlying fascia were retracted from the skull. The skull was adjusted so that bregma and lambda were in the same horizontal plane. To minimize pulsation during the recording session, cerebrospinal fluid was released by puncturing the atlanto-occipital membrane. Small holes were drilled in the skull for the placement of recording and stimulating electrodes. Bipolar stimulating electrodes consisted of enamel-coated stainless-steel wires (100 μm in diameter; California Fine Wire, Grover Beach, CA) with a tip separation of approximately 100 μm and in vitro impedances of 10–30 kΩ. Stimulating electrodes were placed in the substantia nigra (2.2 mm anterior to lambda, 2.0 mm lateral from lambda, 7.5 mm ventral from the brain surface). Arrays of three to four electrodes were placed in the frontal cortex (2.5–3.2 mm anterior to bregma, 0.5–3 mm lateral from bregma, 2–4 mm ventral from the brain surface). Stimulating electrodes were affixed to the skull with dental acrylic. A hole was drilled above the recording site (0.0–1.5 mm posterior to bregma, 2.5–3.0 mm lateral from bregma), and recordings were obtained 6–9 mm ventral from the brain surface.

Electrophysiological recording

Recording electrodes were constructed from borosilicate glass capillaries (2 mm; World Precision Instruments, Sarasota, FL) by using a Narashige vertical pipette puller. Electrodes were filled with 2.5–5% biocytin in 0.5 M NaCl. Tips of the electrodes were broken under microscopic control to 0.5–1.5 μm, yielding in vitro impedances of 15–30 MΩ at 135 Hz. Electrical signals were amplified 10× with an Axoprobe 1A amplifier (Axon Instruments, Foster City, CA) or a Neurodata IR-283 amplifier (Neurodata Instruments Corp., New York, NY) and then further amplified 100× and filtered (500–10,000 Hz) with a custom-built amplifier/filter circuit. The filtered signals were visualized on a standard oscilloscope, digitized on-line (RC Electronics, Inc., Santa Barbara, CA or DataWave Technologies Corp., Longmont, CO) and recorded on magnetic tape for off-line analysis.

Stimuli were generated by a constant-current stimulus isolation unit (World Precision Instruments or Winston Electronics, Millbrae, CA), with timing provided by a microcomputer or a Winston A-65 timer (Winston Electronics). Stimuli were single, monophasic square wave pulses 1–2 mA, 200 μs in duration, and delivered at 0.4 Hz.

Data analysis

Extracellular recordings of action potentials were played back from magnetic tape and analyzed off-line with a Macintosh equipped with a National Instruments (Austin, TX) MIO16L multifunction board. Spontaneous firing was characterized by the following analyses: firing rate, first-order interspike interval histograms, and autocorrelograms. The pattern of spontaneous firing was classified into one of three types based on the autocorrelograms: regular, random, or bursty. Neurons exhibiting two or more regularly spaced peaks (times of increased firing probability) in the autocorrelograms were classified as regular firing; neurons exhibiting an initial, single peak in the autocorrelogram that decayed to a steady state were classified as bursty firing; and neurons whose autocorrelogram ascended smoothly to a steady state were classified as random firing (Perkel et al., 1967; Tepper et al., 1995). Skewness of the interspike interval histogram and coefficient of variation of the interspike interval were determined to provide additional information about the spontaneous firing (Ferguson and Takane, 1989; Cohen, 1996). Antidromic activation was determined by one response per stimulus, and invariant response latency and collision extinction of the antidromic response were determined with appropriately timed spontaneous action potentials (Fuller and Schlag, 1976).

Electrophysiological measures were calculated by using Microsoft Excel (version 7.0). Statistical analyses were performed with Statview with $\alpha = 0.05$ (version 4.02, Abacus Concepts, Inc., Berkeley, CA). Numbers in the text and tables represent mean ± S.E.M.

Juxtacellular labeling and histology

Following electrophysiological characterization, basal forebrain cells were stained juxtacellularly with biocytin (Pinault, 1994). Biocytin was ejected from the recording micropipette with positive current pulses, 2–10 nA, by

using a 50% duty cycle (300 ms on, 300 ms off) for 2–10 minutes through the bridge circuitry of an Axoclamp or Neurodata IR-283 amplifier. Following a survival period of at least 1 hour, rats were perfused with 250 ml of isotonic saline followed by 250 ml each of two ice-cold fixatives (Somogyi and Takagi, 1982). The first fixative consisted of 4% paraformaldehyde, 15% picric acid, and 0.05% glutaraldehyde in 0.1M phosphate buffer (PB; pH 7.4). The second fixative consisted of 4% paraformaldehyde and 15% picric acid in 0.1 M PB (pH 7.4). Brains were removed and postfixed overnight in the second fixative. Coronal sections through the basal forebrain region were cut at 20–25 µm on a Vibratome® (Energy Beam Sciences, Agawam, MA). Sections through the frontal cortex and substantia nigra were cut at 100 µm and processed with Neutral Red or Cresyl Violet for localization of stimulating and recording electrode tracts.

Immunocytochemistry

Three stages were used to process basal forebrain sections for visualization of biocytin and choline acetyltransferase immunoreactivity (ChAT-ir). The first stage consisted of treating alternate sections for biocytin detection by using a modification of the standard method (Horikawa and Armstrong, 1988). All reagents were prepared in 0.1 M PB (pH 7.2). Three 5-minute washes in PB occurred between each step. Brain sections were incubated at room temperature in 0.1 M glycine for 5 minutes, followed by 0.5% hydrogen peroxide for 5 minutes. Tissue was then continuously agitated in an avidin-biotin-peroxidase complex (1:200, standard ABC kit, Vector Laboratories, Inc., Burlingame, CA) solution containing 0.5% Triton X-100 for 2 hours at room temperature or 14–18 hours at 4°C. The next step was an incubation in a solution containing 0.05% 3,3′-diaminobenzidine tetrahydrochloride (DAB) and 0.038% nickel ammonium sulfate for 20 minutes. Hydrogen peroxide was added to the DAB/nickel solution to a final concentration of 0.01%, and the tissue was agitated for another 5–10 minutes. Incubation in 0.01% osmium tetroxide for 10 minutes was followed by mounting on gelatin-coated slides, air drying, dehydration, clearing, and coverslipping. The sections containing portions of the biocytin-labeled cell body or proximal dendrites were located. This stage identified cells that were characterized electrophysiologically and labeled with biocytin.

Untreated tissue sections adjacent to those containing the biocytin-labeled cell body or proximal dendrites were processed for double visualization of biocytin and ChAT-ir. Brains for six rats were processed as follows. The presence of ChAT-ir was determined by using a rat monoclonal anti-ChAT IgG (1:10 with 0.5% Triton X-100; Boehringer Mannheim, Indianapolis, IN; for 12–16 hours at room temperature) and a goat anti-rat IgG-CY3 (1:100; Jackson ImmunoResearch Laboratories, Inc., West Grove, PA; for 2 hours at room temperature). Neurons containing ChAT-ir were located by using fluorescence microscopy and photographed. The sections were further processed to visualize biocytin by using the procedure described for the first processing stage. Photographs were taken, and the presence or absence of ChAT-ir in the biocytin-labeled neuron was determined by a comparison of photographs.

For the remaining rats, the second stage of processing consisted of the following steps. ChAT-ir and biocytin were visualized by using two different fluorophores. Sections were incubated in rat monoclonal anti-ChAT IgG (1:10 with 0.5% Triton X-100; Boehringer Mannheim) for 12–16 hours at room temperature, followed by goat anti-rat IgG-CY3 (1:100; Jackson ImmunoResearch), streptavidin-7-amino-4-methylcoumarin-3-acetic acid (1:100; Jackson ImmunoResearch) and 0.5% Triton X-100 for 2 hours at room temperature. Sections were examined with fluorescence microscopy, and a determination was made concerning the colocalization of biocytin and ChAT-ir. Photomicrographs were taken for documentation. Sections were incubated in biotinylated peroxidase (1:200, 'B' component of standard ABC kit, Vector Laboratories) with 0.5% Triton X-100 for 2 hours at room temperature. The remaining steps were identical to those described for the first processing stage, continuing after the ABC incubation.

The third stage of processing was to incubate the remaining tissue sections with the reagents for visualization of biocytin, as described for the first processing stage.

Bulk injection of biocytin

To verify that our immunocytochemical procedures were compatible with visualization of colocalized biocytin and ChAT-ir, a large extracellular injection of biocytin was made in the SI of one rat. A glass microelectrode was filled with 5% biocytin in 0.5 M NaCl. The tip of the microelectrode was broken to 10 µm in diameter under microscopic control. Biocytin was injected by applying constant positive current (10 µA) for 10 minutes. The rat was killed and the brain was processed as described for the second stage of the immunocytochemical procedure.

Image analysis

Biocytin-labeled neurons were reconstructed with a 40× or 63× objective lens by using a computerized image analysis system (Neurolucida, MicroBrightField, Inc., Colchester, VT). In some cases, neurons were reconstructed by using a drawing tube on a Zeiss or Aus Jena microscope.

Digital photomicrographs were taken with a Kodak DCS-420 digital camera or conventional 35-mm negatives were digitized by a Polaroid SprintScan 35. The digitized images were cropped and adjusted in Adobe Photoshop 3.0. To enhance the images, adjustments in brightness and contrast were made, and an unsharp mask filter was applied. Images were printed by using Adobe Photoshop 3.0 and a dye sublimation printer (Primera Pro, Fargo Electronics, Inc., Iden Prairie, MN).

RESULTS

Morphological characterization

Following the bulk injection, 1,601 neurons in the SI were labeled with biocytin (Fig. 1C). Eighty-nine of these neurons were also shown to be ChAT-ir (Fig. 1D, arrow). These results demonstrate that the immunocytochemical procedures used in the present study were sufficiently sensitive to detect the colocalization of biocytin and ChAT and that fewer than 6% of the neurons in the SI were cholinergic neurons.

Juxtacellular labeling with biocytin was attempted in 59 cells; 39 of these cells were labeled and recovered successfully (66% success rate). In each case, only a single cell was labeled. Of these 39 cells, immunocytochemistry for the presence of ChAT was performed in 17 cells. All 17 cells were ChAT immunonegative (Figs. 1A,B, Table 1). Four

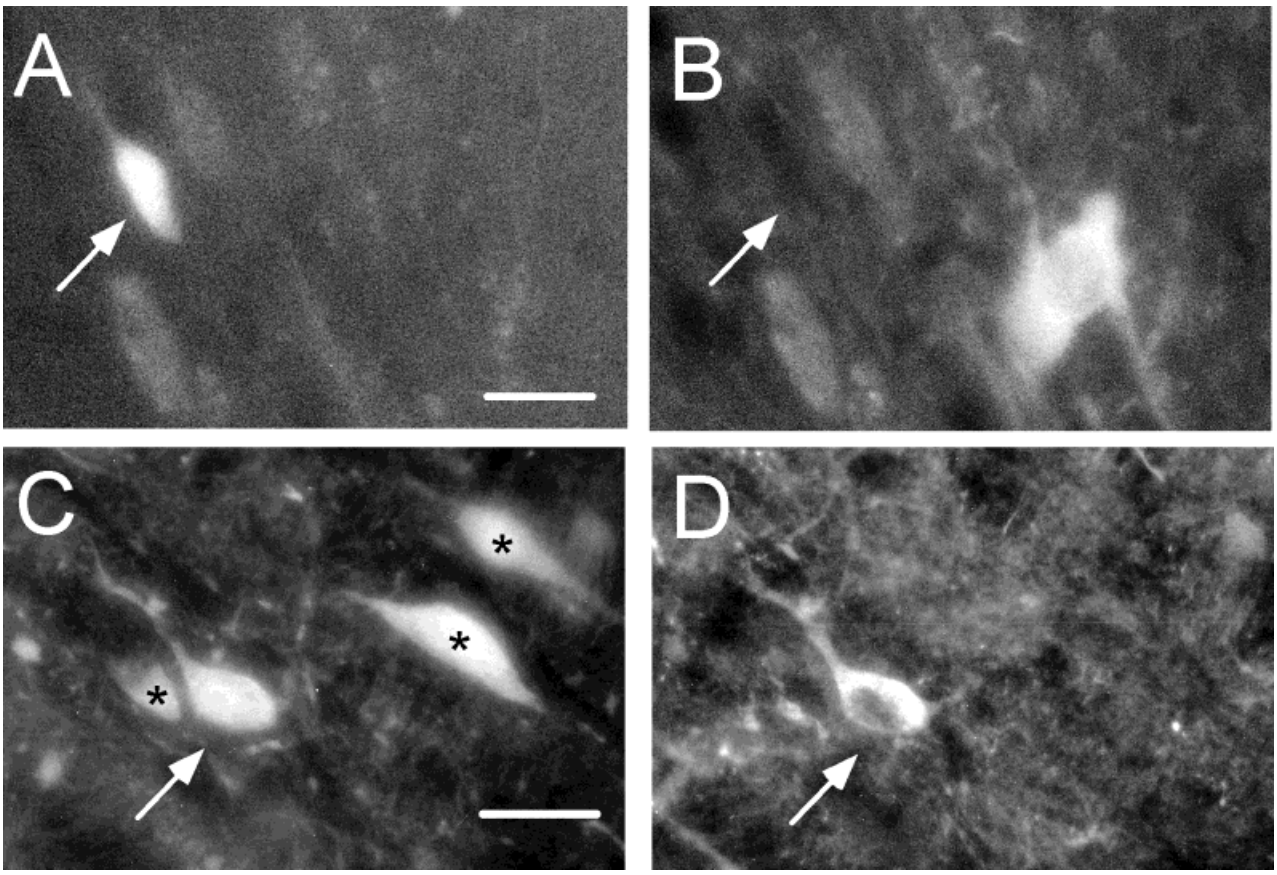

Fig. 1. **A,B:** Biocytin-filled noncholinergic neuron (cell 4) in the ventral pallidum. The neuron was labeled juxtacellularly with biocytin (arrow in A) and was identified as a noncholinergic neuron based on the absence of choline acetyltransferase immunoreactivity (ChAT-ir; arrow in B). **C,D:** Cholinergic neuron in the substantia innnominata. A large, bulk injection of biocytin into the substantia innominata labeled cholinergic (arrow in C and D) and noncholinergic (asterisks in C) neurons. Cholinergic neurons were distinguished by the presence of ChAT-ir (arrow in D). Scale bars = 20 μm.

additional neurons were labeled with biocytin and demonstrated an abundant local axonal arborization within the basal forebrain, a characteristic that is not observed in cholinergic cells (Armstrong, 1986; Zaborszky, 1992). Therefore, these four cells were identified as putative noncholinergic neurons even though ChAT immunocytochemistry was not performed. The locations of the 17 identified noncholinergic neurons and the four putative noncholinergic neurons are depicted in Figure 2. The morphological and electrophysiological characteristics of these neurons are described below and summarized in Tables 1 and 2.

Pallidal neurons. Nine neurons were located in the ventral globus pallidus or VP (Table 1, Fig. 2). Seven of these neurons were demonstrated to be ChAT immunonegative. The two remaining neurons, although not examined for ChAT-ir, issued many local axon collaterals and were thus classified as putative noncholinergic neurons (Fig. 4). A striking feature of pallidal neurons in the present study was that they fell into two groups based on their axonal arborization pattern. One group of pallidal neurons (type I) had relatively simple axons that rarely branched in the vicinity of the soma (Fig. 3). A second group (type II) had complex, highly branched local axon arborizations (Fig. 4).

Five pallidal neurons were classified as type I (Fig. 3, Table 2, cells 1–5). These neurons were small to medium sized, with mean somatic dimensions of 20.4 ± 2.1 μm (long axis) × 10.0 ± 1.4 μm (perpendicular to long axis). Four of the five neurons had oval cell bodies that issued two to five primary dendrites. The dendritic arbor was 1.0 ± 0.1 mm × 0.4 ± 0.1 mm. Three of the five neurons had distinct orientations with the cell bodies and main dendritic axes oriented in an oblique mediolateral direction (Fig. 3A–C). The primary dendrites were thick and originated from opposite poles of the cell body. Each of the primary dendrites branched to form two to three secondary dendrites. The higher order dendrites were moderately spiny in two neurons (Fig. 3A,C) and aspiny in the other neuron (Fig. 3B). The secondary and tertiary dendrites had a varicose appearance (Fig. 3-A2) with a few pedunculated spines (Fig. 3-A3). The remaining two cells of this group exhibited a symmetrical radiating dendritic pattern. The primary dendrites were smooth and bifurcated into two varicose and aspiny secondary dendrites. Axons of all neurons in this group rarely branched and exhibited a few en passant varicosities with long, smooth intervaricose segments. Three neurons had axons that originated from the cell body (Fig. 3B,C), whereas two had axons emanating from the proximal dendrite (Fig. 3-A1). Neuron 2 issued an axon collateral about 150 μm from the axon initial segment (Fig. 3B).

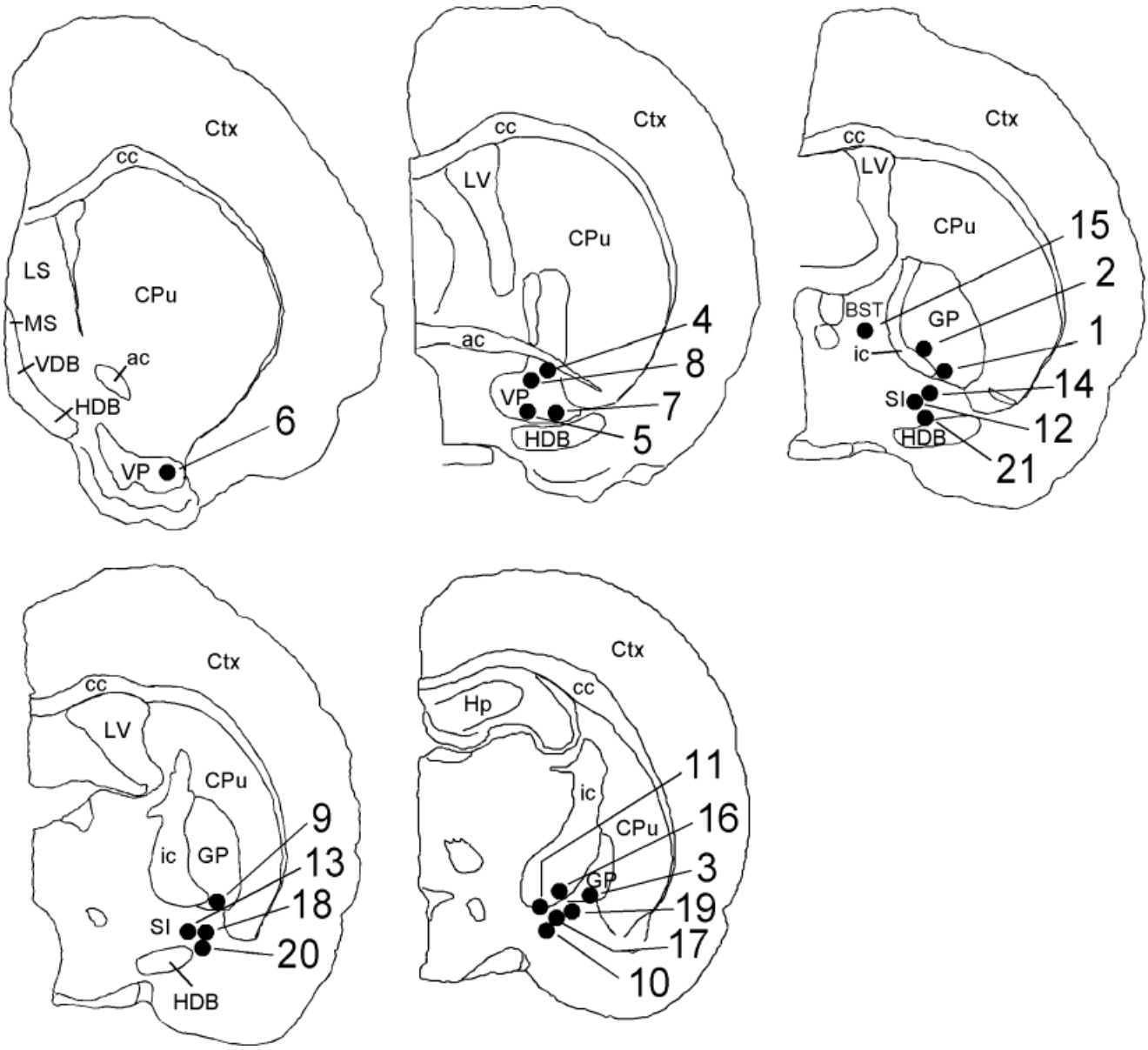

Fig. 2. Rostrocaudal series of schematic coronal sections depicting the locations of juxtacellularly labeled basal forebrain neurons. The numbers represent the neuron identification as designated in Tables 1 and 2. ac, anterior commissure; BST, bed nucleus of the stria terminalis; cc, corpus callosum; CPu, caudate-putamen; Ctx, neocortex; GP, globus pallidus; HDB, horizontal limb of the diagonal band of Broca; Hp, hippocampus; ic, internal capsule; LS, lateral septum; LV, lateral ventricle; MS, medial septum; SI, substantia innominata; VDB, vertical limb of the diagonal band of Broca; VP, ventral pallidum.

In contrast, pallidal type II neurons displayed a relatively rich system of local axon collaterals (Fig. 4, Table 2, cells 6–9). These neurons had medium-sized cell bodies (25.8 ± 3.0 μm × 15.3 ± 3.0 μm) that tended to be larger than those of pallidal type I neurons (20.4 ± 2.1 μm × 10.0 ± 1.4 μm), although this comparison did not reach statistical significance ($t[7] = 1.99$, $P = 0.09$). Three to six primary dendrites originated from the soma, forming a dendritic arbor of 0.7 ± 0.1 mm × 0.5 ± 0.1 mm. Neither the number of primary dendrites nor the area of the dendritic field was significantly different from pallidal type I neurons. Three neurons had asymmetrical dendritic trees (Fig. 4A,B). The fourth neuron had a radiating dendritic field. Primary dendrites were generally smooth and thick and gave rise to two to three secondary dendrites. The secondary dendrites of two neurons were varicose (Fig. 4-A1), and dendritic spines were observed in three neurons (Fig. 4-B1). The axons of all neurons in this group branched frequently, forming a large dense terminal field (Fig. 4A,B). In the three neurons with asymmetrical dendritic fields, the local axonal fields were similarly asymmetrical, generally occupying areas devoid of stained dendrites. The one neuron with a radiating dendritic pattern had a similarly radiating axonal field. Both en passant and terminal axonal varicosities were observed in all cells of this class (Fig. 4-A2,B2). In some cases, large boutons were

TABLE 1. Morphology of Noncholinergic Basal Forebrain Neurons[1]

Cell number	Site	Immuno-reactivity, ChAT	Cell body		Dendrite				Axon
			Size[2] (μm)	Shape	No.[3]	Size[4] (mm)	Shape[5]	Spines[6]	
1	vGP	—	20 × 8	Oval	5	0.8 × 0.5	Disk	10–15	Unbranched, few en passant varicosities
2	vGP	—	25 × 11	Oval	4	1.3 × 0.3	Cylinder	None	Two branches, few varicosities
3	vGP	—	14 × 14	Round	3	0.8 × 0.6	Radiate	Few	Unbranched, few en passant varicosities
4	VP	—	20 × 7	Oval	3	1.2 × 0.2	Disk	20–24	Unbranched, few en passant varicosities
5	VP	—	23 × 10	Oval	2	0.9 × 0.6	Radiate	Few	Unbranched, smooth
6	VP		22 × 12	Triangular	4	0.6 × 0.4	Radiate	Variable	Rich local arbor, en passant and terminal varicosities
7	VP	—	22 × 12	Oval	4	0.7 × 0.5	Radiate	Few	Rich local arbor, en passant and basketlike varicosities
8	VP	—	26 × 14	Oval	3	0.4 × 0.2	Disk	None	Rich local arbor, en passant and basketlike varicosities
9	vGP		33 × 23	Stellate	6	1.0 × 0.8	Radiate	10	Rich arbor, en passant and terminal varicosities
10	SI	—	16 × 8	Oval	2	0.7 × 0.4	Disk	Few	Unbranched, followed into internal capsule
11	SI	—	32 × 12	Oval	4	0.7 × 0.4	Radiate	15	Unbranched, followed into internal capsule
12	SI	—	15 × 10	Oval	4	1.0 × 0.6	Radiate	Few	Unbranched
13	SI	—	20 × 12	Oval	4	0.7 × 0.7	Radiate	None	Unbranched, followed 2 mm from soma
14	SI	—	20 × 16	Multipolar	5	0.7 × 0.5	Radiate	None	Unbranched
15	BST	—	11 × 7	Oval	3	0.7 × 0.6	Radiate	10–15	Unbranched
16	SI		22 × 15	Triangular	2	0.8 × 0.7	Radiate	None	Few local collaterals, followed 1 mm from soma
17	SI	—	20 × 15	Triangular	4	0.6 × 0.3	Radiate	10	Few local collaterals with varicosities
18	SI	—	47 × 17	Fusiform	6	1.1 × 0.6	Radiate	None	Few local collaterals, few en passant varicosities
19	SI	—	15 × 8	Oval	4	0.6 × 0.5	Radiate	None	Few local collaterals
20	SI		18 × 6	Triangular	3	0.6 × 0.5	Radiate		Rich local arborization
21	SI	—	17 × 13	Oval	4	0.9 × 0.7	Radiate	10–40	Rich local arborization, en passant varicosities

[1]SI, substantia innominata; vGP, ventral globus pallidus; VP, ventral pallidum; BST, bed nucleus of stria terminalis.
[2]Longest and shortest diameter.
[3]Number of primary dendrites.
[4]Approximate length of the longest and the perpendicular axis of the dendritic field.
[5]Shape of the dendritic field.
[6]Spine number/100 μm.

TABLE 2. Electrophysiology of Noncholinergic Basal Forebrain[1]

Cell number	Site and cell type	AP duration (ms)	Spontaneous activity			
			Firing rate (Hz)	ISI skewness	ISI CV	Pattern
1	vGP, type I	2.4	5.2	1.53	0.552	Random
2	vGP, type I	2.6	25.5	2.99	0.310	Regular
3	vGP, type I	2.4	32.2	0.63	0.215	Regular
4	VP, type I	2.8	2.8 (907)	3.38	1.034	Random
5	VP, type I	1.6	0.5 (247)	1.51	0.863	Random
6	VP, type II	1.8	16.4	1.95	0.510	Random
7	VP, type II	2.3	51.4	0.84	0.222	Regular
8	VP, type II	2.5	35.1	0.81	0.213	Regular
9	vGP, type II	3.2	39.1	0.63	0.153	Regular
10	SI	2.3	4.8 (957)	4.03	0.892	Random
11	SI	2.2	0.7 (331)	2.57	0.997	Bursty
12	SI	2.4	6.0 (823)	2.54	0.767	Random
13	SI	2.7	13.6 (1825)	5.25	0.726	Random
14	SI	2.4	22.6	0.35	0.271	Regular
15	BST					
16	SI	2.0	2.46 (1062)	2.21	0.834	Random
17	SI	2.2	6.9	4.75	1.378	Random
18	SI	2.4	29.1	2.94	0.610	Random
19	SI	2.1	3.1 (993)	3.38	1.305	Bursty
20	SI	2.2	35.2	2.97	1.306	Bursty
21	SI	2.3	15.4 (1867)	1.95	0.61	Random

[1]SI, substantia innominata; vGP, ventral globus pallidus; VP, ventral pallidum; BST, bed nucleus stria terminalis; AP, action potential; CV, coefficient of variation; ISI, interspike interval. A total of 2,001 spikes were used to calculate spontaneous firing measures unless noted in the parenthesis after the firing rate.

observed on the axon collaterals, with grapelike terminals surrounding unstained cell bodies (Fig. 4-A2).

Substantia innominata neurons. Eleven neurons were located in the SI and one was recorded in the bed nucleus of the stria terminalis. Ten of these neurons were ChAT immunonegative. The remaining two neurons were not identified immunocytochemically but had local axon collaterals, a feature not present in cholinergic neurons. In contrast to pallidal neurons, SI neurons did not fall into discrete groups based on local axon arborization. Instead, these neurons formed a continuum. Some neurons had unbranched axons (Fig. 5), others had moderate axonal branching (Fig. 6), and the remaining cells had profuse local axonal branching (Fig. 7).

The general features of SI neurons are described in Table 1. Substantia innominata neurons were small to medium-sized cells with mean soma dimensions of 21.1 ± 2.9 μm × 11.6 ± 1.1 μm. Oval-shaped cell bodies were the most common (Fig. 7A), but various other cell body shapes were noted, including multipolar, triangular (Fig. 6A,B), and fusiform. Two to six primary dendrites originated from the cell body, the dendritic arbor extended 0.8 ± 0.05 mm × 0.5 ± 0.04 mm, and all except one exhibited a radiating pattern. Dendrites ranged from aspiny (Fig. 6-A1) to sparsely spiny and moderately spiny (Figs. 5-B2, 6B, 7B). Dendritic varicosities were observed in some neurons, mostly on distal dendrites (Fig. 6-A1,A2). The local axonal arborization of SI neurons varied considerably. Six neurons showed no axonal collaterals in the vicinity of the soma (Fig. 5). Two of the axons of these neurons could be observed entering the internal capsule (numbers 10 and 11), one was traced toward the external capsule (number 13), one was activated antidromically by stimulation of the frontal cortex (number 12), and two neurons were antidromically activated by stimulation of the substantia nigra (numbers 16 and 21). Four SI neurons had a few collaterals near the soma (Fig. 6), and two cells (numbers 20 and 21) had a moderately dense local axon collateral plexus in the vicinity of their cell bodies (Fig. 7). These axonal arbors often extended beyond the dendritic field of the neurons (Fig. 7). However, the axonal branching of these last two SI neurons did not appear to be as rich as those observed in the pallidal type II neurons, and axons of these neurons extended beyond the dendritic field in contrast to pallidal type II neurons. Both en passant and terminal varicosities were observed on axons of SI neurons (Figs. 5-B1, 6-A2, 6-B1, 7C).

Comparisons between pallidal and substantia innominata neurons. Soma area, dendritic area, and number of primary dendrites did not differ significantly between either of the VP subpopulations and SI neurons. However, qualitative morphological differences were

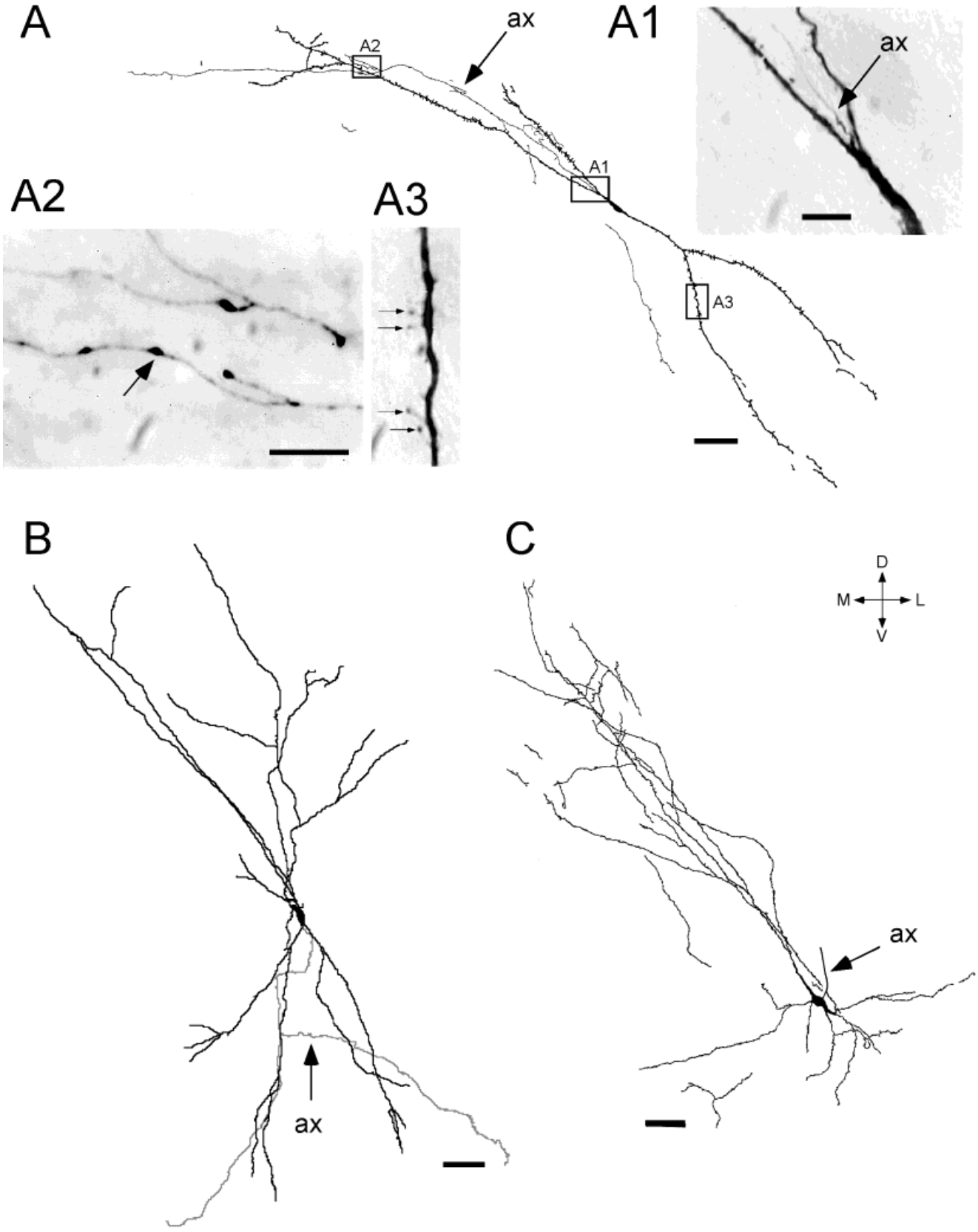

Fig. 3. Three examples of type I pallidal cells. Camera lucida reconstructions of neurons 4 (**A**) and 1 (**C**) and the computer-assisted reconstruction of neuron 2 (**B**) illustrate the oblique dendritic field and cell body orientations that were common for this class of cells. These cells had axons (ax) that could be followed for long distances from the soma and had few local axon collaterals. In **A1**, the axon (arrow) emerged from the first branch point of a primary dendrite and displayed en passant varicosities in the distal region (arrow in **A2**). Spines were present on proximal and distal dendrites (arrows in **A3**). Neurons in Figures 3–7 were sectioned in the coronal plane. Orientation guide: D, dorsal; V, ventral; M, medial; L, lateral. Scale bars = 50 µm in A–C, 10 µm in A1–A3.

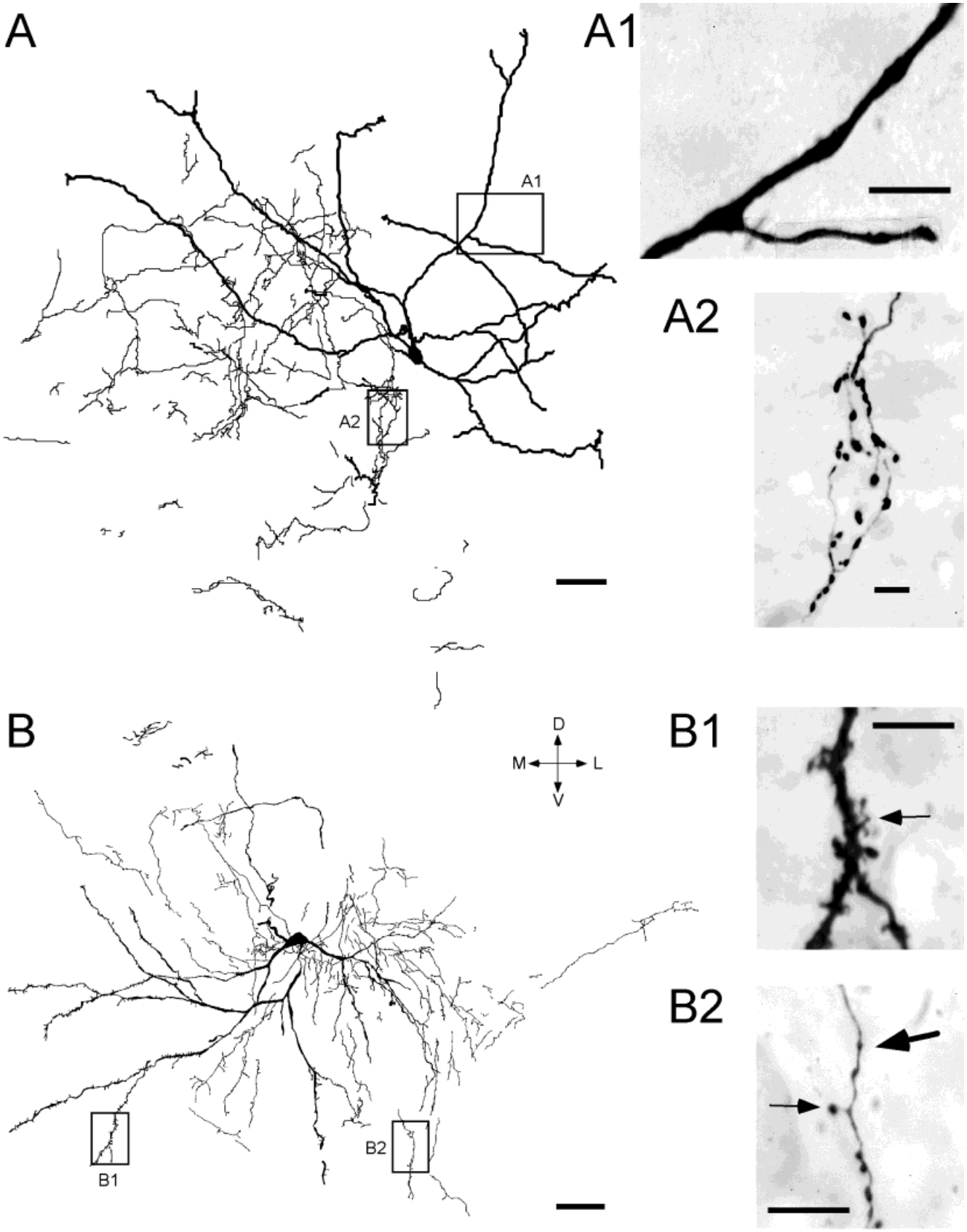

Fig. 4. Two examples of type II pallidal neurons. Computer reconstruction of one neuron (**A**, cell 7) and camera lucida drawing of another (**B**, cell 6) show the prolific local axon branching that was typical of this class. Note the moderately varicose dendrites in **A1**. The axon contained large en passant and terminal boutons, sometimes surrounding unstained cell bodies (**A2**). In **B1**, the distal dendrites of another neuron exhibited spines and stout protrusions (arrow) and axons had both terminal (**B2**, small arrow) and en passant varicosities (B2, large arrow). Scale bars = 50 µm in A,B, 10 µm in A1,A2,B1,B2.

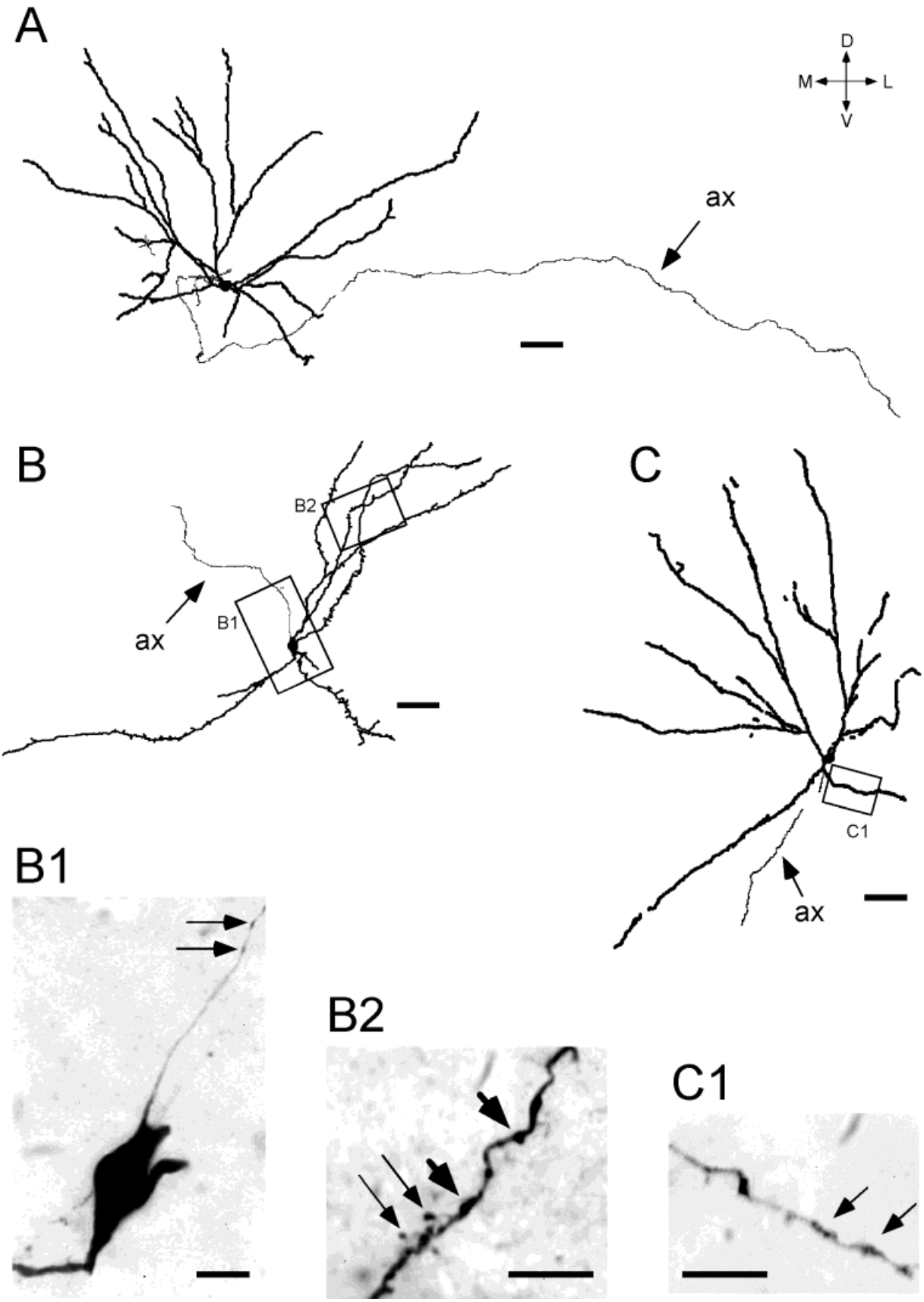

Fig. 5. Three examples of substantia innominata cells with axons that rarely branched in the vicinity of the soma. Computer reconstruction of neurons 13 (**A**), 11 (**B**), and 12 (**C**) demonstrate the scarcity of local axon collaterals that was characteristic of this type of neuron. The main axons (ax) were followed for long distances from the cell body. Dendrites of some substantia innominata neurons were varicose (arrowheads in **B2**, arrows in **C1**), with occasional spines (B2, small arrows). The axon originated from the soma and exhibited en passant varicosities (**B1**, arrows). Scale bars = 50 µm in A–C, 10 µm in B1,B2,C1.

observed between the pallidal type II neurons and the SI neurons with extensive intranuclear axonal branching.

Electrophysiological characterization

The electrophysiological properties of noncholinergic pallidal and SI neurons are summarized in Table 2. All neurons except two had positive–negative–positive triphasic action potential waveforms as illustrated for two representative VP neurons (Fig. 8A,B) and one SI neuron (Fig. 8C). The two exceptions (cells 5 and 9; not shown) had biphasic positive–negative waveforms. Spontaneous firing rates ranged from 0.5–51.4 spikes/second. One of 11 neurons (number 12) was activated antidromically from frontal cortex, and 2 of 17 cells (numbers 16 and 21; Fig. 8D) were activated antidromically from the substantia nigra.

Pallidal neurons. As described in the previous section, pallidal neurons could be divided into two groups based on anatomical features. These two types of pallidal neurons had the following electrophysiological characteristics. Pallidal type I neurons had a mean spontaneous firing rate of 13.2 ± 7.3 Hz and an action potential duration of 2.4 ± 0.2 ms. All exhibited positive–negative–positive triphasic action potential waveforms (Fig. 8-B3) with one exception (number 5) that had a positive–negative biphasic waveform. The distribution of first-order interspike intervals was characterized by a skewness of 2.01 ± 0.57 and a coefficient of variation of 0.595 ± 0.175. Three neurons had random spontaneous firing patterns (Fig. 8B) and two had a regular pattern. None of the pallidal type I neurons was activated antidromically by frontal cortex (n = 0/1) or substantia nigra (n = 0/4) stimulation.

Pallidal type II neurons tended to have a higher spontaneous firing rate than did pallidal type I neurons, although this comparison did not quite reach statistical significance (35.5 ± 8.4 Hz, t[7] = 2.285, $P = 0.056$). The mean action potential duration was 2.5 ± 0.3 ms with all neurons except one having a triphasic action potential waveform (Fig. 8). The exception had a biphasic positive–negative waveform. The skewness of the interspike interval distribution was 1.06 ± 0.35 and the coefficient of variation was 0.275 ± 0.092. Three pallidal type II neurons fired spontaneously in a regular pattern (Fig. 8A), whereas the remaining neuron fired randomly. Action potential duration, skewness, coefficient of variation, and firing pattern did not differ significantly between type I and II pallidal neurons. None of the pallidal type II neurons was activated antidromically from frontal cortex (n = 0/2) or substantia nigra (n = 0/2) stimulation.

Substantia innominata neurons. Substantia innominata neurons had spontaneous firing rates of 12.7 ± 3.7 Hz (n = 11) and action potential durations of 2.3 ± 0.1 ms. All action potentials displayed a positive–negative–positive triphasic waveform (Fig. 8-C4). Skewness and coefficient of variation of the first-order interspike intervals were 2.99 ± 0.43 and 0.881 ± 0.109, respectively. Seven SI neurons exhibited a random firing pattern, and one showed a regular pattern and three exhibited bursting (Fig. 8C). One SI neuron (number 12), which issued an unbranched axon, was driven antidromically from frontal cortex (n = 1/8) with a latency of 5.6 ms. The conduction velocity was estimated to be 0.71 m/second by using a straight line distance between stimulation and recording electrodes. Two other neurons, one with few local axon collaterals and the other with a rich local axon arbor, were driven antidromically from substantia nigra (n = 2/11) with latencies of 10 ms (number 16, Fig. 8D) and 8.9 ms (number 21). Axonal conduction velocities for these neurons were estimated to be 0.47 and 0.75 m/second, respectively.

Comparisons between pallidal and substantia innominata neurons. Certain electrophysiological characteristics differed between pallidal type II neurons and SI neurons. Spontaneous firing rates were lower for SI neurons than for pallidal type II neurons (t[13] = 3.151, $P < 0.01$) and the firing pattern was less regular for SI neurons than for pallidal type II neurons as seen by the more skewed interspike interval histogram (t[13] = 2.704, $P < 0.05$) and the higher coefficient of variation (t[13] = 3.344, $P < 0.01$). A significant difference in the distribution of firing patterns was found between these two groups of neurons ($\chi^2[2] = 6.690$, $P < 0.05$). Electrophysiological properties did not differ between pallidal type I and SI neurons.

DISCUSSION

The morphological and electrophysiological characteristics of noncholinergic basal forebrain neurons were determined and correlated in the present study. Seventeen neurons were identified as noncholinergic based on the absence of ChAT-ir. Four neurons were classified as putative noncholinergic neurons based on the abundant local axon collaterals (Armstrong, 1986; Zaborszky, 1992). The major findings of the present study are as follows. (1) Noncholinergic VP neurons could be subdivided into two groups based on the axonal arborization pattern, cell size, and spontaneous firing rates. Type I neurons, which had few local axon collaterals, discharged at a relatively low spontaneous firing rate and may represent projection neurons, whereas type II neurons, which had rich en passant and basketlike varicosities, exhibited a high spontaneous firing rate and may correspond to interneurons. (2) Substantia innominata neurons had local axon collaterals that varied gradually from none to profuse, with local axonal arborizations generally extending beyond the dendritic field. Neurons with both branched and unbranched axons were observed to send main axons into the internal capsule, external capsule, and/or could be activated antidromically from either the frontal cortex or substantia nigra, suggesting that these neurons are projection neurons. (3) Pallidal neurons with extensive local axon arbors had electrophysiological characteristics quite different from those of SI neurons.

Morphological and electrophysiological characterization of basal forebrain and pallidal neurons

The morphology of globus pallidus and basal forebrain neurons in rodents and primates has been studied extensively by using the Golgi stain (Fox et al., 1974; Danner and Pfister, 1981; Iwahori and Mizuno, 1981; DiFiglia et al., 1982; Francois et al., 1984; Millhouse, 1986; Brauer et al., 1988). These studies have described in great detail the variability of dendritic arborization with respect to pattern and special features. However, the classification of cells by using the Golgi technique does not usually involve axonal characteristics because of the incomplete impregnation of the axons with this technique. Thus, a convincing morphological characterization of basal forebrain neurons has been difficult with this technique. Although in vitro intracellular recordings (Alonso et al., 1996; Nambu and Llinas,

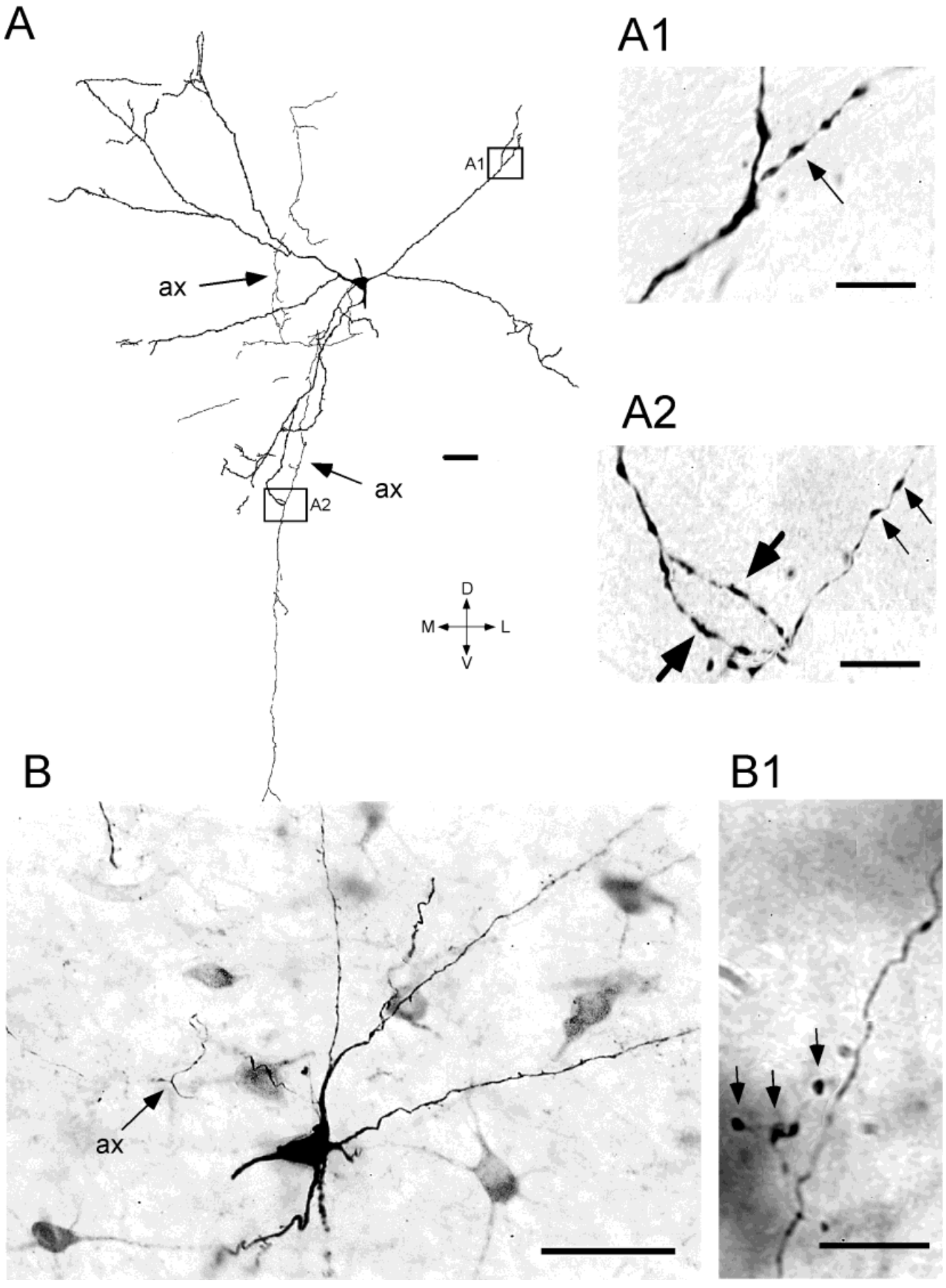

Figure 6

1997) have revealed much about the intrinsic electrophysiological properties of these neurons, in vitro intracellular staining often does not allow a complete morphological reconstruction of the neurons. In vivo intracellular studies without morphological reconstruction (Lavin and Grace, 1996) or chemical identification (Park et al., 1982; Semba et al., 1987; Kita and Kitai, 1994) also prevent a definitive conclusion as to the identity of the neurons. The in vivo juxtacellular labeling, as used in the present study, offers several advantages over that used in other studies. In addition to the study of the entire somatodendritic morphology, the axons in most cases can be completely reconstructed or can be identified by antidromic activation. Moreover, the spontaneous firing properties of the neuron can be easily assessed without concern that the intracellular impalement may have altered the neuron's spontaneous firing rate or pattern. This technique in combination with immunocytochemical methods has the potential to identify the neurochemical characteristics of the recorded neuron. The yield of labeled cells is greater using juxtacellular labeling than when using intracellular labeling. However, although it has been hypothesized that the recorded and labeled neuron is the same after juxtacellular labeling in all cases (Pinault, 1994), it is nearly impossible to prove this unequivocally. The fact that in every case only a single extracellular spike train was recorded and only a single neuron was labeled following juxtacellular iontophoresis of biocytin lends support to the idea that this labeling technique does in fact label the neuron that was being recorded.

Ventral pallidal neurons

Pallidal neurons have been classified based on the cell size, dendritic specializations (spines, complex endings, appendages), axonal arborization, spatial orientation of the dendritic tree, and electrophysiological characteristics. Although a recent intracellular study (Kita and Kitai, 1994) found no systematic association between somatic size and dendritic or axonal morphology, the present study suggests that pallidal neurons may be subdivided into two classes: type I pallidal neurons were those with few intranuclear axon branches, and type II neurons were those with rich local axonal arbors. Moreover, although not statistically significant, type II pallidal neurons tended to be larger than pallidal type I cells, suggesting a possible relationship between somatic size and axon morphology.

It is apparent that the dendritic arborization of pallidal neurons is similar in primates and rodents and shows a systematic relationship to the pallidal borders. In three-dimensional computer reconstructions, the dendritic arbor of most pallidal neurons in the rostrolateral region correspond to a flat disk, whereas the dendrites of other neurons, especially in more medial and caudal parts of the rodent globus pallidus, have cylindrical or radiating dendritic fields (Park et al., 1982; Percheron et al., 1984; Yelnik et al., 1984; Millhouse, 1986; Kita and Kitai, 1994). Our data agree with the observations that VP neurons (including ventral globus pallidus neurons) have disklike, cylindrical, or radiating dendritic fields. A previous report suggested that neurons with cylindrical or conical dendritic fields exhibited dendritic spines, whereas cells with disklike dendritic fields did not (Kita and Kitai, 1994). In contrast, our data did not indicate any association between the presence or absence of spines and any other obvious morphological features, such as somatic size, or the axonal or dendritic arborization pattern, which is consistent with the observation of Millhouse (1986). In a few cases, we observed preterminal and terminal dendritic appendages (Fig. 4-B1), noted previously both in primates and rodents (DiFiglia et al., 1982; Francois et al., 1984; Millhouse, 1986; Kita and Kitai, 1994).

According to Golgi and intracellular staining studies, most rodent pallidal neurons emit one or a few short, sparsely branched intranuclear axon collaterals with sparse-to-moderate en passant and terminal boutons (Iwahori and Mizuno, 1981; Park et al., 1982; Millhouse, 1986). A recent intracellular staining study of pallidal projection neurons described two types of axonal arborization patterns. Aspiny neurons emitted multiple collaterals in the globus pallidus (e.g., N-37 in Fig. 5 of Kita and Kitai, 1994), which branched infrequently and displayed only sparsely distributed boutons. Sparse-to-moderately spiny neurons exhibited frequent local axonal branching forming a dense terminal field that extended beyond the dendritic field of the parent neuron (e.g., N-6 in Fig. 5 of Kita and Kitai, 1994). Based on the limited number of well-stained axons in the present study, it may be premature to generalize about the differences in the axonal fields of spiny and aspiny globus pallidus neurons. However, it is apparent that our neuron 2, which was located in the ventromedial part of the globus pallidus, is similar to the pallidal projection neuron N-37 of Kita and Kitai (1994). Our neuron 2 had a relatively large soma, aspiny dendrites, an axon collateral emanating from the main axon at about 150–200 μm from the cell body and a cylindrical dendritic field. In contrast, the profuse intranuclear axon branching of our pallidal type II neurons (Fig. 4) resembled neuron N-6 of Kita and Kitai (1994), which projected to the subthalamic nucleus. Based on morphological features, pallidal type I and II neurons in our study may correspond to the two types of pallidal projection neurons described by Kita and Kitai (1994). However, some morphological differences were also noted between our type II neurons and the spiny projection neurons of Kita and Kitai (1994). For example, type II neurons in the present study had axonal arborizations that could not be traced beyond the dendritic tree and that showed many basketlike terminals (Fig. 4-A2). In fact, the pallidal type II neurons of the present study may correspond to the small spine-bearing neurons with circumscribed dendritic trees and rich local axonal arborizations that have been observed in Golgi studies of the primate and rodent globus pallidus (Fox et al., 1974; Danner and Pfister, 1981; DiFiglia et al., 1982; Francois et al., 1984) or the type III pallidal neurons of Nambu and Llinas (1997, Fig. 6) in the guinea pig. These neurons were considered to be interneu-

Fig. 6. Examples of substantia innominata cells with moderately branched axons. Camera lucida drawing of cell 16 (**A**) and photomicrograph of cell 17 (**B**) illustrate the long main axon (ax) and the moderately branching local axon plexus that was common for cells in this class. Distal dendrites of cell 16 were varicose (**A1**, arrow; **A2**, large arrows). The axonal varicosities (A2, small arrows) were smaller than the dendritic varicosities. Cell 17 (B, black neuron) is shown among cholinergic neurons in the background (light grey cells). Dendritic spines were present, mostly in the distal regions. En passant varicosities were observed on the axon with clusters (**B1**, arrows) forming near cholinergic (B1, the cholinergic cell is visible as a dark patch near the arrows) and unidentified cells. Scale bars = 50 μm in A,B, 10 μm in A1,A2,B1.

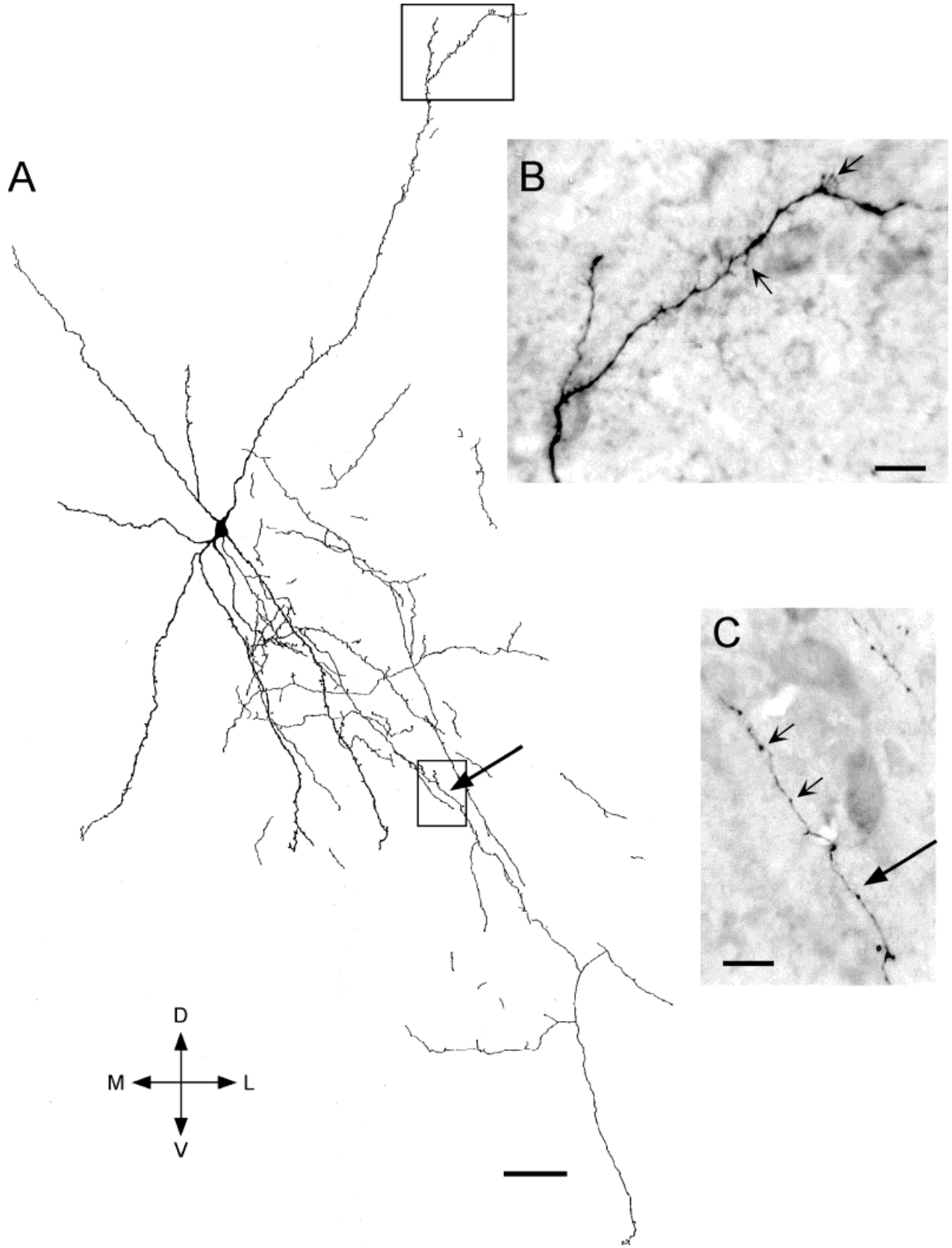

Fig. 7. A substantia innominata neuron with a highly branched local axon collateral arbor. **A:** Camera lucida drawing of cell 21. **B:** Distal dendrites were mildly varicose and moderately spiny. Some pedunculated spines were observed (arrows). The local axon collateral system was extensive but not as rich as type II pallidal neurons (compare with Fig. 4). In addition, the local collaterals of this type of substantia innominata neuron generally extended past the dendritic arbor, in contrast to type II pallidal cells. En passant axonal varicosities were abundant (**C**, small arrows). The arrow in A points to the axon in C (large arrow). Scale bars = 50 µm in A, 10 µm in B,C.

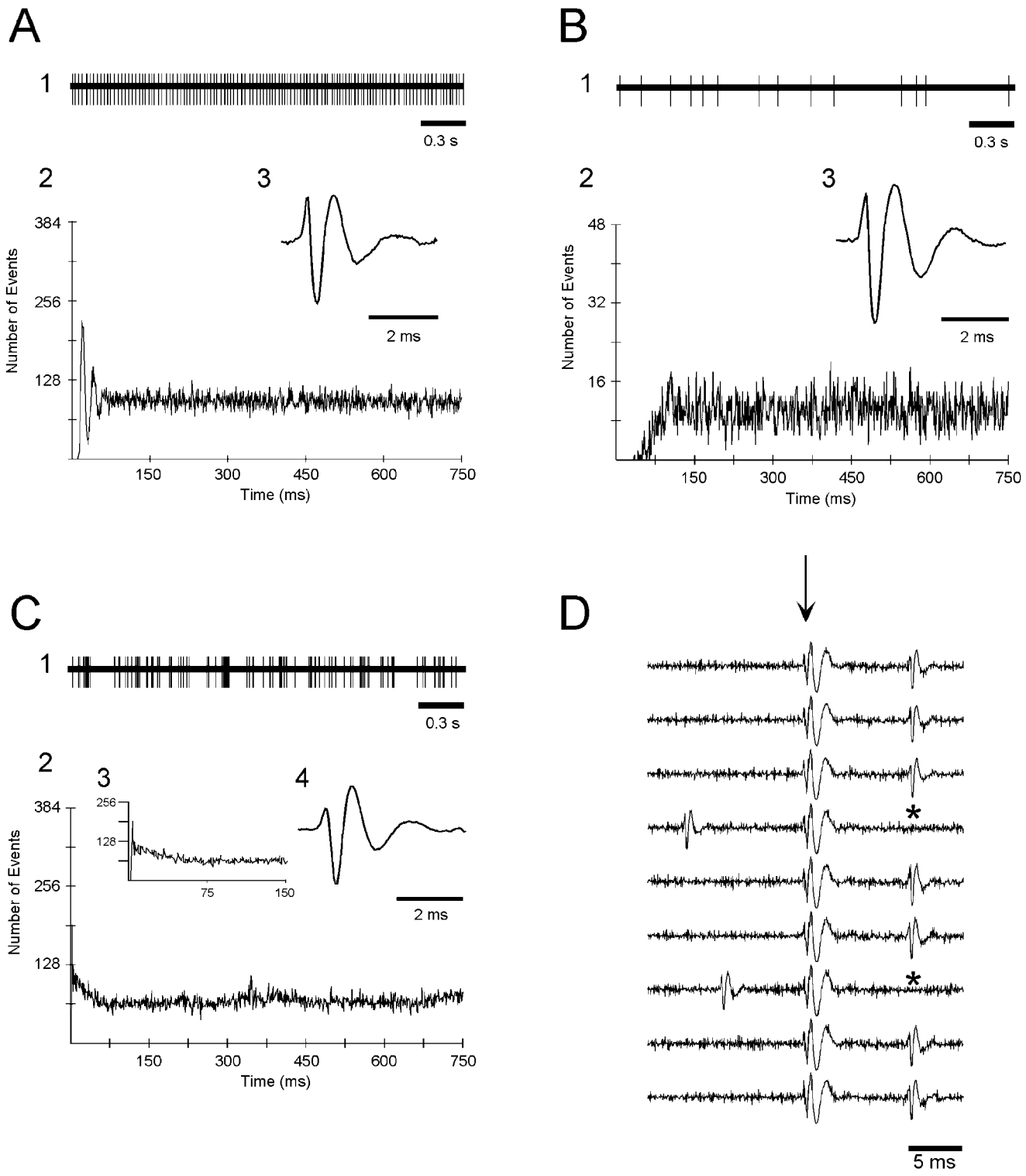

Fig. 8. Extracellular recordings of a neuron with regular firing (**A**, cell 7), one with random firing (**B**, cell 1), and one with bursty firing (**C**, cell 20). Regular firing was observed in the raw spike train (**A1**) and by the multiple peaks in the autocorrelogram (**A2**). Random firing was denoted by the irregular pattern of firing in the spike train (**B1**) and the lack of peaks in the autocorrelogram (**B2**). A bursty firing pattern was noted by the clustering of action potentials in the spike train (**C1**) and the single peak decaying to a steady state in the autocorrelogram (**C2**). An expanded view of the initial portion of the autocorrelogram is shown in **C3**. The action potential was triphasic with a positive–negative–positive waveform in all cases (**A3,B3,C4**). Bin width was 1 ms for all autocorrelograms, and each autocorrelogram was generated from 2,001 spikes. A substantia innominata projection neuron was activated antidromically by stimulation of the substantia nigra (**D**, cell 16). Nine consecutive sweeps are shown. Antidromic activation was determined by the constant latency of activating an action potential, collision with spontaneous action potentials (asterisk in sweeps 4 and 7), and ability to follow at high stimulation frequencies (not shown). The start of the stimulus artifact is marked with an arrow. Stimulus pulses were 1.5 mA, 200 μs. Positivity is upward for the oscilloscope tracings.

rons by those investigators. Thus, our pallidal type I neurons are likely to be projection neurons, whereas pallidal type II neurons may be either projection neurons or interneurons. Regardless of whether pallidal type II neurons are projection neurons or interneurons, it is clear from the morphology that these neurons represent different functional elements for information processing in the VP. Based on morphological considerations, type I neurons might be expected to have little influence on neighboring cells, whereas type II neurons should have significant impact on the activity of other cholinergic or noncholinergic neurons in the near vicinity.

Several recent extra- and intracellular recording studies in rodents have suggested that cholinergic neurons in the basal forebrain show a periodic burst firing pattern, although the transmitter content of the recorded neurons in most cases was not identified (Griffith and Matthews, 1986; Khateb et al., 1992; Lavin and Grace, 1996; Nunez, 1996; Brazhnik and Fox, 1997). In the present study, none of our noncholinergic pallidal neurons displayed a bursty pattern of spontaneous firing. Thus, our results are consistent with the idea that cholinergic pallidal neurons have bursty spontaneous firing patterns, whereas noncholinergic neurons do not. However, this feature of cholinergic and noncholinergic neurons may not generalize to other basal forebrain areas because we and others (Alonso et al., 1996) have observed that noncholinergic neurons in the SI can discharge in a bursty firing pattern.

Studies using intracellular recording of neurons in the globus pallidus and the VP have described three types of neurons (Kita and Kitai, 1991; Lavin and Grace, 1996; Nambu and Llinas, 1997). One neuronal type was spontaneously active, had spontaneous firing rates of 10–20 Hz, and discharged in single action potentials as opposed to bursts. This neuronal population may include the type I pallidal neurons of the present study, the type II globus pallidus neurons of Nambu and Llinas (1997), the repetitive firing globus pallidus neurons of Kita and Kitai (1991), and the type B ventral pallidal neurons of Lavin and Grace (1996). Action potential duration did not differ between type I and II pallidal neurons of our study, in contrast to what would be expected from a previous study (Lavin and Grace, 1996). However, the lack of differences in the present study may be attributed to the use of extracellular recordings versus intracellular recordings. Thus, pallidal type I neurons of the present study may correspond to the type B ventral pallidal neurons of Lavin and Grace (1996) and may provide a morphological description for these putative GABAergic neurons. In addition, VP neurons had similar electrophysiological and morphological characteristics to previously described globus pallidus neurons.

Type II VP neurons of the present study had some similarities to type III globus pallidus neurons of Nambu and Llinas (1997). Both fired in single spike firing patterns. However, type III neurons of Nambu and Llinas (1997) were not active spontaneously, and our type II VP neurons had the highest firing rates of all neurons in the study. These differences may be due to the different preparations used (i.e., in vitro vs. in vivo). Intracellular recordings showed that type III globus pallidus neurons of Nambu and Llinas (1997) had characteristics similar to type A ventral pallidal neurons of Lavin and Grace (1996). Thus, the morphological description of type II VP neurons in the present study may correspond to the electrophysiological characteristics found in type A ventral pallidal neurons, tentatively suggested to be GABAergic neurons (Lavin and Grace, 1996). The morphological and elecytrophysiological characteristics of pallidal neurons from the present and previous studies are summarized in Table 3.

Substantia innominata neurons

Basal forebrain areas, including the horizontal limb of the diagonal band, SI, and internal capsule, contain most of the corticopetal cholinergic neurons and have been the focus of several Golgi (Brauer et al., 1988; Dinopoulos et al., 1988) and intracellular labeling (Reiner et al., 1987; Semba et al., 1987; Alonso et al., 1996) studies. Based on the cell size, dendritic surface structures and presence of dendritic spines, Brauer et al. (1988) classified neurons in the SI into five categories: SI-NB I was identified as cholinergic in a subsequent immunohistochemical study (Brauer et al., 1991), and SI-NB II–V morphological types were tentatively identified as GABAergic.

Recent studies have indicated that immunocytochemistry for the calcium-binding proteins, parvalbumin (PV), calretinin (CR), and calbindin (CB), labels subpopulations of GABAergic neurons in many areas of the brain, including basal forebrain areas (Cullinan and Zaborszky, 1989; Freund, 1989; Celio, 1990; Jacobowitz and Winsky, 1991; Rogers, 1992; Kawaguchi et al., 1995). The percentages of the different GABAergic subpopulations vary across brain regions. The most abundant GABAergic neuronal population in the SI contains CB, followed by CR and PV. CR- and CB-containing neurons had small soma sizes, whereas PV-containing neurons were larger (Zaborszky et al., unpublished observations). However, PV-containing neurons consisted of two distinct populations differing in soma size. Based on cell size alone, cells 10, 12, 15, 19, and 20 may be CR-, CB- or small PV-containing neurons. However, neurons 12–14 were immunonegative for PV-ir. In addition, spines are rarely observed on PV-ir dendrites (Kita, 1994), and therefore, neurons 11, 15, 17, and 21 are unlikely to be PV-immunopositive neurons. Basal forebrain neurons may also contain peptides such as somatostatin or neuropeptide Y, both of which are found in basal forebrain local neurons that innervate adjacent cholinergic projection neurons with symmetric synapses (Zaborszky, 1989). In any event, the correspondence between peptidergic content and morphology of SI neurons must await future studies.

In the present study, SI neurons could not be easily subdivided based on axonal or dendritic morphology. Local axon collaterals of these neurons ranged from none to profuse. However, even those neurons with rich local axon collaterals did not appear to have axonal arbors as rich as pallidal type II neurons. Almost all of the SI neurons had radiating dendritic fields. Half of the neurons were aspiny, whereas the rest were bestowed with few to moderate numbers of spines. Spiny cell 21 in our study (Fig. 7) had similar dendritic/axonal arborization patterns and spine densities to cell 2 of Reiner et al. (1987) and Semba et al. (1987). Both neurons were projection neurons; the neuron in Reiner et al. (1987) projected to the frontal cortex, and the cell in the present study projected caudally toward the substantia nigra. However, the size of the cell body in Reiner et al. (1987) was much larger (42 μm longest diameter) than the one in our study (17 μm), which could be due to different labeling and processing techniques. In summary, although previous morphological studies have identified multiple subpopulations of SI neurons, the

TABLE 3. Characteristics of Pallidal Neurons

Noncholinergic neurons of ventral pallidum and ventral globus pallidus in present study			Neurochemically unidentified neurons in the ventral pallidum or globus pallidus in previous studies	
Dendrite	Axon	Electrophysiology	Morphology, location[1]	Electrophysiology[2]
Discoidal, cylindrical, or radiate; aspiny and moderately spiny	No or infrequent branching, few local boutons	13.2 Hz; random or regular	Type II of Nambu and Llinas[3] (1997, in vitro, GP): moderately spiny, few local collaterals, project to the striatum. N-37 of Kita and Kitai[4] (1994, in vivo, GP): aspiny, discoidal dendritic field, infrequent local collaterals, project to the subthalamic nucleus. Millhouse[4] (1986, Golgi, GP): radiate or compressed dendritic trees, some axons with collaterals and numerous en passant varicosities. Park et al.[4] (1982, in vivo, GP): medial neurons with cylindrical dendritic trees, sparsely spiny, no axon collaterals; lateral neurons with disk-shaped dendritic trees, sparsely spiny, a few axon collaterals. Iwahori and Mizuno[5] (1981, Golgi, GP): straight dendrites spread in radial fashion, some axons bifurcated and had a few intranuclear collaterals.	Type II neuron of Nambu and Llinas[3] (1997, in vitro, GP): fired at resting membrane level, repetitive firing to small membrane depolarization. Type B neuron of Lavin and Grace[4] (1996, in vivo, VP): 14.5 Hz, prominent AHP. Repetitive firing neuron of Kita and Kitai[4] (1991, in vivo, GP): 50–130 Hz maximum firing, spike accomodation.
Radiate; sparse to moderately spiny	Frequent branching, rich local terminal or en passant boutons, often basketlike arborization	35.5 Hz; mostly regular	Type III of Nambu and Llinas[3] (1997, in vitro, GP): small spiny, rich local collaterals, probable interneuron. N-6 projection neuron of Kita and Kitai[4] (1994, in vivo, GP): sparsely spiny neuron with radiate dendritic tree and rich local terminal field. Danner and Pfister[4] (1981); Fox et al.[6] (1974); DiFiglia et al.[6] (1982); Francois et al.[6] (1984): small spine bearing neuron with circumscribed dendritic tree, rich local axonal arborization (Golgi studies, GP), probable interneuron.	Type III neuron of Nambu and Llinas[3] (1997, in vitro, GP): fired repetitively at a low frequency upon direct depolarization with weak or no accomodation. Type A of Lavin and Grace[4] (1996, in vivo, VP): phasic spikes that did not exhibit substantial AHP, 8.7 Hz.

[1]VP, ventral pallidum; GP, globus pallidus.
[2]AHP, after-hyperpolarization.
[3]Guinea pig.
[4]Rat.
[5]Mouse.
[6]Monkey.

morphological analysis of axonal arborization in the present study was unable to classify clearly these neurons into separate groups.

Extracellular recordings of neurochemically unidentified basalocortical neurons have revealed a wide range of spontaneous firing rates (0–40 Hz), different types of spontaneous firing patterns (bursty, random, and regular), and antidromic conduction velocities (Aston-Jones et al., 1984, 1985; Lamour et al., 1986; Nunez, 1996). The quite variable electrophysiological properties may result from recordings of different types of neurons within the SI. In vitro intracellular recordings identified two types of neurons in the SI. Cholinergic neurons fired in either bursts or tonic patterns depending on the membrane potential just prior to depolarization (Alonso et al., 1996). Bursts of action potentials occurred on top of low-threshold spikes and a very prominent and long-lasting after-hyperpolarization occurred after an action potential. In vivo extracellular recordings from unidentified SI neurons have also demonstrated a population of cells with bursty firing patterns that changed to tonic firing with cortical electroencephalographic (EEG) desynchronization (Nunez, 1996). These neurons were suggested to be cholinergic. In vitro intracellular recordings also demonstrated that noncholinergic neurons discharged in clusters of action potentials (Alonso et al., 1996). However, the firing of noncholinergic neurons had distinctive differences from cholinergic neurons. Noncholinergic neurons did not exhibit low-threshold spiking, and had short after-hyperpolarizations and rapid rates of firing. In vivo extracellular recordings of putative noncholinergic neurons demonstrated a short duration action potential and a tonic and regular firing pattern (Nunez, 1996). These neurons did not fire in bursts and decreased their firing rates with cortical EEG desynchronization. In general, cholinergic neurons in the SI appear to discharge in bursts and have a wide action potential duration with a long-lasting after-hyperpolarization, leading to a relatively low firing rate. Two populations of noncholinergic neurons may exist, one of which displays a bursty firing pattern and the other firing in a tonic, regular pattern.

In the present study, 7 of 11 electrophysiologically characterized SI neurons showed a random firing pattern. One neuron exibited moderately regular firing, whereas the remaining three SI neurons exhibited bursting activity. These latter three neurons may correspond to the burst firing population of noncholinergic neurons reported previously (Alonso et al., 1996). It must also be noted that the burst firing observed in the present study was more modest than that observed in previous studies (compare the autocorrelogram of Fig. 8-C2 in the present study with Fig. 2-D of Nunez, 1996). The firing rate of SI neurons in the present study (mean = 12.7 Hz) was very similar to the tonic neurons reported in a recent extracellular study of basal forebrain neurons (12.1 Hz: Nunez, 1996).

At least 6 of 12 SI neurons in the present study were projection neurons because they were activated antidromically from frontal cortex or substantia nigra and/or because their axons could be traced into the internal or external capsule. The estimated conduction velocities were 0.47–0.75 m/second. Given that these velocities were calculated based on the straight line distance between stimulation and recordings electrodes, it is highly likely that our calculated conduction velocities significantly underestimate the true values. These estimates are on the low end of the previously reported conduction velocities of unidentified nucleus basalis neurons (0.6–9.1 m/second; Aston-Jones et al., 1984, 1985; Lamour et al., 1986; Detari and Vanderwolf, 1987) but are consistent with reported conduction velocities of neostriatal medium-sized GABAergic projection neurons (Richardson et al., 1977; Ryan et al., 1986). Antidromic activation was observed in SI neurons with few intranuclear axon branches and with those cells with rich branching. Thus, both types are projection cells, lending support to the idea that unbranched and branched SI neurons may constitute a heterogeneous population. The characterization of SI neurons into subpopulations, therefore, awaits further, more sophisticated morphological and electrophysiological studies.

Functional considerations

Morphological and electrophysiological analyses of noncholinergic basal forebrain neurons have provided evidence for differences between VP and SI. VP noncholinergic neurons could be clearly segregated into two subpopulations based on intranuclear axon branching, which seem to correspond to intracellularly characterized VP neurons of Lavin and Grace (1996). The morphological characteristics of VP neurons in our study were similar to globus pallidus neurons reported previously (Table 3), suggesting that VP neurons, with their specifically oriented dendritic fields, could integrate topographically organized inputs. In contrast to the dorsal main body of the globus pallidus, however, VP neurons receive input from ventral striatal areas, including the nucleus accumbens, and from the basolateral amygdala and prefrontal cortex (Zaborszky et al., 1984, 1997; Sesack et al., 1989; for review, see Heimer et al., 1991). The VP, like its dorsal counterpart, projects to the entopeduncular nucleus, substantia nigra, and mesencephalic locomotor area, structures belonging to what has been traditionally termed the 'extrapyramidal motor system.' However, a substantial outflow of VP efferents is directed to the ventral tegmental area, mediodorsal nucleus (MD) of the thalamus, medial prefrontal cortex, basolateral amygdala, and entorhinal cortex (Haber et al., 1985; Groenwegen et al., 1993), structures belonging to 'limbic' circuits integrating cognitive reward-related signals with motor output elements (Mogenson et al., 1993). Cholinergic VP neurons that receive input from the nucleus accumbens and project to the amygdala (Zaborszky et al., 1984; Carlsen et al., 1985) have also been implicated in the development of drug addiction (White and Hiroi, 1993). Additionally, GABAergic VP neurons that project to the MD of the thalamus and the posterior lateral hypothalmus (Zahm et al., 1987; Gritti et al., 1994) may indirectly modulate the excitability of the cerebral cortex (Mancia et al., 1993).

In contrast to VP neurons, many of the noncholinergic SI neurons in the present study were similar to the 'isodendritic' (Ramon-Moliner and Nauta, 1966) or generalized type of dendritic arbor (Valverde, 1961; Ramon-Moliner, 1962) neurons in the reticular formation of the brainstem. Similarities between SI and reticular formation neurons were found in the long Golgi type I axon, with a variety of local axonal arborization patterns, the lack of true Golgi type II neurons in the SI (present study; Scheibel and Scheibel, 1958; Leontovich and Zhukova, 1963), and overlapping dendritic fields (Brauer et al., 1988). All of these results support the notion that basal forebrain areas, including the SI and horizontal limb of the diagonal band, represent a cephalic continuation of the brainstem reticular formation (Leontovich and Zhukova, 1963). These noncholinergic neurons of the SI could receive attentional, arousal, or reward-related input from the locus coeruleus and substantia nigra as indicated by previous morphological studies (Zaborszky et al., 1993; Zaborszky and Cullinan, 1996; Gaykema and Zaborszky, 1997). Thus, noncholinergic, putative GABAergic projection neurons in the SI with their local collaterals, overlapping dendritic fields, and widespread cortical projections (Saper, 1984; Grove, 1988) may offer an optimal substrate for a coordinated modulatory system that acts on different cortical areas according to the prevailing state of the animal. Recent studies combining microdialysis of cortical acetylcholine, electrical recording in different cortical areas, and basal forebrain stimulation suggest a complex control of cortical activity by a mechanism involving both GABAergic and cholinergic projection neurons of the basal forebrain (Jimenez-Capdeville et al., 1997).

ACKNOWLEDGMENTS

The technical assistance of Mr. Alvaro Duqué and Mr. Paul Anderson is greatly acknowledged.

LITERATURE CITED

Alonso, A., A. Khateb, P. Fort, B.E. Jones, and M. Muhlethaler (1996) Differential oscillatory properties of cholinergic and non-cholinergic nucleus basalis neurons in guinea pig brain slice. Eur. J. Neurosci. *8:*169–182.

Armstrong, D.M. (1986) Ultrastructural characterization of choline acetyltransferase-containing neurons in the basal forebrain of rat: Evidence for a cholinergic innervation of intracerebral blood vessels. J. Comp. Neurol. *250:*81–92.

Asanuma, C. and L.L. Porter (1990) Light and electron microscopic evidence for a GABAergic projection from the caudal basal forebrain to the thalamic reticular nucleus in rats. J. Comp. Neurol. *302:*159–172.

Aston-Jones, G., R. Shaver, and T. Dinan (1984) Cortically projecting nucleus basalis neurons in rat are physiologically heterogeneous. Neurosci. Lett. *46:*19–24.

Aston-Jones, G., R. Shaver, and T.M. Dinan (1985) Nucleus basalis neurons exhibit axonal branching with decreased impulse conduction velocity in rat cerebrocortex. Brain Res. *325:*271–285.

Brauer, K., A. Schober, J.R. Wolff, E. Winkelmann, H.-J. Luth, and H. Bottcher (1991) Morphology of neurons in the rat basal forebrain nuclei: Comparison between NADPH-diaphorase histochemistry and immunocytochemistry of glutamic acid decarboxylase, choline acetyltransferase, somatostatin and parvalbumin. J. Hirnforsch. *32:*1–17.

Brauer, K., W. Schober, L. Werner, E. Winkelmann, W. Lungwitz, and F. Hajdu (1988) Neurons in the basal forebrain complex of the rat: A Golgi study. J. Hirnforsch. *29:*43–71.

Brazhnik, E.S. and S.E. Fox (1997) Intracellular recordings from medial septal neurons during hippocampal theta rhythm. Exp. Brain Res. *114:*442–453.

Carlsen, J., L. Zaborszky, and L. Heimer (1985) Cholinergic projections from the basal forebrain to the basolateral amygdaloid complex: A combined retrograde fluorescent and immunohistochemical study. J. Comp. Neurol. *234:*155–167.

Celio, M.R. (1990) Calbindin D-28k and parvalbumin in the rat nervous system. Neuroscience *35:*375–475.

Chan-Palay, V., M. Hochli, S. Savaskan, and G. Hungerecker (1993) Calbindin D-28k and monoamine oxidase A immunoreactive neurons in the nucleus basalis of Meynert in senile dementia of the Alzheimer's type and Parkinson's disease. Dementia *4:*1–15.

Cohen, B.H. (1996) Explaining Psychological Statistics. Albany: Brooks/Cole.

Cullinan, W.E. and L. Zaborszky (1989) Afferents to calcium-binding protein containing basal forebrain neurons. Soc. Neurosci. Abstr. *15:* 999.

Danner, H. and C. Pfister (1981) Untersuchungen zur Zytoarchitektonik des Globus Pallidus der Ratte. J. Hirnforsch. *22:*47–57.

Detari, L. and C.H. Vanderwolf (1987) Activity of identified cortically projecting and other basal forebrain neurones during large slow waves and cortical activation in anaesthetized rats. Brain Res. *437:*1–8.

DiFiglia, M., P. Pasik, and T. Pasik (1982) A Golgi and ultrastructural study of the monkey globus pallidus. J. Comp. Neurol. *212:*53–75.

Dinopoulos, A., J.G. Parnavelas, H.B.M. Uylings, and C.G. van Eden (1988) Morphology of neurons in the basal forebrain nuclei of the rat: A Golgi study. J. Comp. Neurol. *272:*461–474.

Ferguson, G.A. and Y. Takane (1989)Statistical Analysis in Psychology and Education. New York: McGraw-Hill Book Company.

Fox, C.A., A.N. Andrade, I.J. LuQui, and J.A. Rafols (1974) The primate globus pallidus: A Golgi and electron microscopic study. J. Hirnforsch. *15:*75–93.

Francois, C.G., G. Percheron, J. Yelnik, and S. Heyner (1984) A Golgi analysis of the primate globus pallidus. I. Inconstant processes of large neurons, other neuronal types and afferent axons. J. Comp. Neurol. *227:*182–199.

Freund, T.F. (1989) GABAergic septohippocampal neurons contain parvalbumin. Brain Res. *478:*375–381.

Fuller, J.H. and J.D. Schlag (1976) Determination of antidromic excitation by the collision test: Problems of interpretation. Brain Res. *112:*283–298.

Gaykema, R.P.A. and L. Zaborszky (1997) Parvalbumin-containing neurons in the basal forebrain receive direct input from the substantia nigra-ventral tegmental area. Brain Res. *478:*375–381.

Geula, C. and M.M. Mesulam (1994) Cholinergic systems and related neuropathological predilection patterns in Alzheimer's disease. In R.D. Terry, B. Katzman, and K.L. Bick (eds): Alzheimer's Disease. New York: Raven Press, pp. 263–291.

Griffith, W.H. and R.T. Matthews (1986) Electrophysiology of AChE-positive neurons in basal forebrain slices. Neurosci. Lett. *71:*169–174.

Gritti, I., L. Mainville, and B.E. Jones (1994) Projections of GABAergic and cholinergic basal forebrain and GABAergic preoptic-anterior hypothalamic neurons to the posterior lateral hypothalamus of the rat. J. Comp. Neurol. *339:*251–268.

Gritti, L., L. Mainville, and B.E. Jones (1993) Codistribution of GABA with acetylcholine synthesizing neurons in the basal forebrain of the rat. J. Comp. Neurol. *329:*438–457.

Groenwegen, H.J., H.W. Berendse, and S.N. Haber (1993) Organization of the output of the ventral striatopallidal system in the rat: Ventral pallidal efferents. Neuroscience *57:*113–142.

Grove, E.A. (1988) Efferent connections of the substantia innominata in the rat. J. Comp. Neurol. *277:*347–364.

Haber, S.N., H.J. Groenewegen, E.A. Grove, and W.J.H. Nauta (1985) Efferent connections of the ventral pallidum: Evidence of a dual striato pallidofugal pathway. J. Comp. Neurol. *235:*322–335.

Heimer, L., J. de Olmos, G.F. Alheid, and L. Zaborszky (1991) 'Perestroika' in the basal forebrain: Opening the border between neurology and psychiatry. Prog. Brain Res. *87:*109–165.

Heimer, L., R.E. Harlan, G.F. Alheid, M.M. Garcia, and J. De Olmos (1997) Substantia innominata: A notion which impedes clinical–anatomical correlations in neuropsychiatric disorders. Neuroscience *76:*957–1006.

Horikawa, K. and W.E. Armstrong (1988) A versatile means of intracellular labeling: Injection of biocytin and its detection with avidin conjugates. J. Neurosci. Methods *25:*1–11.

Ingham, C.A., J.P. Bolam, and A.D. Smith (1988) GABA-immunoreactive synaptic boutons in the rat basal forebrain: Comparison of neurons that project to the neocortex with pallidosubthalamic neurons. J. Comp. Neurol. *273:*263–282.

Iwahori, N. and N. Mizuno (1981) A Golgi study of the globus pallidus of the mouse. J. Comp. Neurol. *197:*29–43.

Jacobowitz, D.M. and L. Winsky (1991) Immunocytochemical localization of calretinin in the forebrain of the rat. J. Comp. Neurol. *304:*198–218.

Jimenez-Capdeville, M.E., R.W. Dykes, and A.A. Myasnikov (1997) Differential control of cortical activity by the basal forebrain in rats: A role for both cholinergic and inhibitory influences. J. Comp. Neurol. *381:*53–67.

Kawaguchi, Y., C.J. Wilson, S.J. Augood, and P.C. Emson (1995) Striatal interneurons: Chemical, physiological and morphological characterization. Trends Neurosci. *18:*527–535.

Khateb, A., M. Muhlethaler, A. Alonso, M. Serafin, L. Mainville, and B.E. Jones (1992) Cholinergic nucleus basalis neurons display the capacity for rhythmic bursting activity mediated by low-threshold calcium spikes. Neuroscience *51:*489–494.

Kita, H. and S.T. Kitai (1991) Intracellular study of rat globus pallidus neurons: Membrane properties and responses to neostriatal, subthalamic and nigral stimulation. Brain Res. *564:*296–305.

Kita, H. and S.T. Kitai (1994) The morphology of globus pallidus projection neurons in the rat: An intracellular staining study. Brain Res. *636:*308–319.

Kita, H. (1994) Parvalbumin-immunopositive neurons in rat globus pallidus: A light and electron microscopic study. Brain Res. *657:*31–41.

Lamour, Y., P. Dutar, O. Rascol, and A. Jobert (1986) Basal forebrain neurons projecting to the rat frontoparietal cortex: Electrophysiological and pharmacological properties. Brain Res. *362:*122–131.

Lavin, A. and A.A. Grace (1996) Physiological properties of rat ventral pallidal neurons recorded intracellularly in vivo. J. Neurophysiol. *75:*1432–1443.

Leontovich, T.A. and G.P. Zhukova (1963) The specificity of the neuronal structure and topography of the reticular formation in the brain and spinal cord of carnivora. J. Comp. Neurol. *121:*347–381.

Mancia, M., M. Mariotti, and I. Gritti (1993) GABAergic synchronizing influences of basal forebrain and hypothalamic preoptic regions on the mediodorsal nucleus of the thalamus. Sleep Res. *22:*444.

Millhouse, O.E. (1986) Pallidal neurons in the rat. J. Comp. Neurol. *254:*209–227.

Mogenson, G.J., M. Brudzynski, M. Wu, C.R. Yang, and C.Y. Yim (1993) From motivation to action: A review of dopaminergic regulation of limbic-nucleus accumbens-ventral pallidum-pedunculopontine nucleus circuitries involved in limbic motor integration. In P.B. Kalivas and C.D. Barnes (eds): Limbic Motor Circuits and Neuropsychiatry. Boca Raton: CRC Press, pp. 193–236.

Muir, J.L., B.J. Everitt, and T.W. Robbins (1994) AMPA-induced excitotoxic lesions of the basal forebrain: A significant role for the cortical cholinergic system in attentional function. J. Neurosci. *14:*2313–2326.

Nambu, A. and R. Llinas (1997) Morphology of globus pallidus neurons: Its correlation with electrophysiology in guinea pig slices. J. Comp. Neurol. *377:*85–94.

Nunez, A. (1996) Unit activity of rat basal forebrain neurons: Relationship to cortical activity. Neuroscience *72:*757–766.

Pang, K., M.J. Williams, H. Egeth, and D.S. Olton (1993) Nucleus basalis magnocellularis and attention: Effects of muscimol infusions. Behav. Neurosci. *107:*1031–1038.

Park, M.R., W.M. Falls, and S.T. Kitai (1982) An intracellular HRP study of the rat globus pallidus. I. Responses and light microscopic analysis. J. Comp. Neurol. *211:*284–294.

Percheron, G., J. Yelnik, and C. Francois (1984) A Golgi analysis of primate globus pallidus. III. Spatial organization of the striato-pallidal complex. J. Comp. Neurol. *227:*214–227.

Perkel, D.H., G.L. Gerstein, and G.P. Moore (1967) Neuronal spike trains and stochastic point processes. I. The single spike train. Biophys. J. *7:*391–418.

Pinault, D. (1994) Golgi-like labeling of a single neuron recorded extracellularly. Neurosci. Lett. *170:*255–260.

Price, D.L., L.J. Martin, S.S. Sisodia, L.C. Walker, M.L. Voytko, M.V. Wagster, L.C. Cork, and V.E. Koliatsos (1994) The aged nonhuman primate. A model for the behavioral and brain abnormalities occurring in aged humans. In R.D. Terry, R. Katzman, and K.L. Bick (eds): Alzheimer's Disease. New York: Raven Press, pp. 231–245.

Ramon-Moliner, E. (1962) An attempt at classifying nerve cells on the basis of their dendritic patterns. J. Comp. Neurol. *119:*211–227.

Ramon-Moliner, E. and W.J.H. Nauta (1966) The isodendritic core of the brain stem. J. Comp. Neurol. *126:*311–336.

Reiner, P.B., K. Semba, H.C. Fibiger, and E.G. McGeer (1987) Physiological evidence for subpopulations of cortically projecting basal forebrain neurons in the anesthetized rat. Neuroscience *20:*629–636.

Richardson, T.L., J.J. Miller, and H. McLennan (1977) Mechanisms of excitation and inhibition in the nigrostriatal system. Brain Res. *127:*219–234.

Robbins, T.W., B.J. Everitt, H.M. Marston, J. Wilkerson, G.H. Jones, and K.J. Page (1989) Comparative effects of ibotenic acid- and quisqualic acid-induced lesions of the substantia innominata on attentional function in the rat: Further implications for the role of the cholinergic neurons of the nucleus basalis in cognitive processes. Behav. Brain Res. *35:*221–240.

Rogers, J.H. (1992) Immunohistochemical markers in rat cortex: Colocalization of calretinin and calbindin-D28k with neuropeptides and GABA. Brain Res. *587:*147–157.

Ryan, L.J., S.J. Young, and P.M. Groves (1986) Substantia nigra stimulation evoked antidromic responses in rat neostriatum. Exp. Brain Res. *63:*449–460.

Saper, C.B. (1984) Organization of cerebral cortical afferent systems in the rat. I. Magnocellular basal nucleus. J. Comp. Neurol. *222:*313–342.

Sarter, M. (1994) Neuronal mechanisms of the attentional dysfunction in senile dementia and schizophrenia: Two sides of the same coin? Psychopharmacology *114:*539–550.

Scheibel, M.E. and A.B. Scheibel (1958) Structural substrates for integrative patterns in the brain stem reticular core. In H.H. Jasper, L.D. Proctor, R.S. Knighton, W.C. Noshay, and R.T. Costello (eds): The Reticular Formation of the Brain. Boston: Little Brown and Company, pp. 31–55.

Semba, K., P.B. Reiner, E.G. McGeer, and H.C. Fibiger (1987) Morphology of cortically projecting basal forebrain neurons in the rat as revealed by intracellular iontophoresis of horseradish peroxidase. Neuroscience *20:*637–651.

Sesack, S.R., A.Y. Deutch, R.H. Roth, and B.S. Bunney (1989) Topographical organization of the efferent projections of the medial prefrontal cortex in the rat: An anterograde tract-tracing study with *Phaseolus vulgaris* leucoagglutinin. J. Comp. Neurol. *290:*213–242.

Somogyi, P. and H. Takagi (1982) A note on the use of picric acid-paraformaldehyde-glutaraldehyde fixative for correlated light and electron microscopic immunocytochemistry. Neuroscience *7:*1779–1784.

Tepper, J.M., L.P. Martin, and D.R. Anderson (1995) $GABA_A$ receptor-mediated inhibition of rat substantia nigra dopaminergic neurons by pars reticulata projection neurons. J. Neurosci. *15:*3092–3103.

Valverde, F. (1961) Reticular formation of the pons and medulla oblongata. A Golgi study. J. Comp. Neurol. *116:*71–99.

Vincent, S.R., T. Hokfelt, L.R. Skirboll, and J.Y. Wu (1983) Hypothalamic gamma-aminobutyric acid neurons project to the neocortex. Science *220:*1309–1311.

Walker, L.C., V.E. Koliatsos, C.A. Kitt, R.T. Richardson, A. Rokaeus, and D.L. Price (1989) Peptidergic neurons in the basal forebrain magnocellular complex of the rhesus monkey. J. Comp. Neurol. *280:*272–282.

Wenk, G.L. (1997) The nucleus basalis magnocellularis cholinergic system: One hundred years of progress. Neurobiol. Learn. Memory *67:*85–95.

White, N.M. and N. Hiroi (1993) Amphetamine conditioned cue preference and neurobiology of drug-seeking. Sem. Neurosci. *5:*329–336.

Yelnik, J., G. Percheron, and C. Francois (1984) A Golgi analysis of the primate globus pallidus. II. Quantitative morphology and spatial orientation of dendritic arborization. J. Comp. Neurol. *227:*200–213.

Zaborszky, L. (1989) Afferent connections of the forebrain cholinergic projection neurons with special reference to monoaminergic and peptidergic fibers. In M. Frotscher and U. Misgeld (eds): Central Cholinergic Synaptic Transmission. Basel: Birkhauser, pp. 12–32.

Zaborszky, L. (1992) Synaptic organization of basal forebrain cholinergic projection neurons. In E.D. Levin, M. Decker, and L. Butcher (eds): Neurotransmitter Interactions and Cognitive Functions. Boston: Birkhauser, pp. 27–65.

Zaborszky, L. and W.E. Cullinan (1996) Direct catecholaminergic-cholinergic interactions in the basal forebrain. I. Dopamine-β-hydroxylase and tyrosine hydroxylase input to cholinergic neurons. J. Comp. Neurol. *374:*535–554.

Zaborszky, L., C. Leranth, and L. Heimer (1984) Ultrastructural evidence for amygdalofugal axons terminating on cholinergic cells of the rostral forebrain. Neurosci. Lett. *52:*219–225.

Zaborszky, L., J. Carlsen, H.R. Brashear, and L. Heimer (1986a) Cholinergic and GABAergic afferents to the olfactory bulb in the rat with special emphasis on the projection neurons in the nucleus of the horizontal limb of the diagonal band. J. Comp. Neurol. *243:*488–509.

Zaborszky, L., L. Heimer, F. Eckenstein, and C. Leranth (1986b) GABAergic input to cholinergic forebrain neurons: An ultrastructural study using retrograde tracing of HRP and double immunolabeling. J. Comp. Neurol. *250:*282–295.

Zaborszky, L., W.E. Cullinan, and V.N. Luine (1993) Catecholaminergic–cholinergic interaction in the basal forebrain. Prog. Brain Res. *98:*31–49.

Zaborszky, L., R.P. Gaykema, D.J. Swanson, and W.E. Cullinan (1997) Cortical input to the basal forebrain. Neuroscience *79:*1051–1078.

Zahm, D.S., L. Zaborszky, G.F. Alheid, and L. Heimer (1987) The ventral striatopallidothalamic projection. II. The ventral pallidothalamic link. J. Comp. Neurol. *255:*592–605.